High-Resolution Near Infrared Spectroscopy and Vibrational Dynamics of Dideuteromethane (CH_2D_2)[†]

O. N. Ulenikov,[‡,§] E. S. Bekhtereva,[‡,§] S. Albert,[‡] S. Bauerecker,[‡,||] H. Hollenstein,[‡] and M. Quack*[,‡]

Physical Chemistry, ETH Zürich, CH-8093 Zürich, Switzerland, Laboratory of Molecular Spectroscopy, Physics Department, Tomsk State University, Tomsk, 634050, Russia, and Technische Universität Braunschweig, D - 38106, Braunschweig, Germany

Received: November 7, 2008; Revised Manuscript Received: December 22, 2008

We report the infrared spectrum of CH_2D_2 measured in the range from 2800 to 6600 cm^{-1} with the Zürich high-resolution Fourier transform interferometer Bruker IFS 125 prototype (ZP 2001, with instrumental bandwidth less than 10^{-3} cm^{-1}) at 78 K in a collisional enclosive flow cooling cell used in the static mode. Precise experimental values (with uncertainties between 0.0001 and 0.001 cm^{-1}) were obtained for the band centers by specific assignment of transitions to the $J = 0$ level of 71 vibrational levels. In combination with 22 previously known band centers, these new results were used as the initial information for the determination of the harmonic frequencies, force constant parameters F_{ij}, anharmonic coefficients, and vibrational resonance interaction parameters. A set of 47 fitted parameters for an effective Hamiltonian reproduces the vibrational level structure of the CH_2D_2 molecule up to 6600 cm^{-1} with a root-mean-square deviation $d_{rms} = 0.67$ cm^{-1}. The results are discussed in relation to the multidimensional potential hypersurface of methane and its vibrational dynamics.

1. Introduction

The vibrational spectroscopy and vibrational dynamics of polyatomic molecules on multidimensional Born−Oppenheimer potential hypersurfaces has been a long standing problem of molecular spectroscopy and molecular physics.[1−3] The traditional approach to relate spectra and properties of potential hypersurfaces has been to start out from the harmonic approximation and to derive anharmonic potential constants in a Taylor series expansion by means of fitting effective Hamiltonians derived from perturbation theory to experimental rovibrational spectra.[4−12] However, it was recognized some time ago that for an accurate description of the relation between spectra, vibrational dynamics, and potential hypersurfaces vibrational (and rovibrational) variational calculations are necessary. Max Wolfsberg and his colleagues have been among the pioneers in this field with early calculations on H_2O and CH_2O[13−16] about a quarter century ago. Over the years numerous calculations of increasing accuracy have been reported for these two semirigid molecules, and we quote here as examples (from a very large literature on the topic) only a few (see ref 17−22 and references cited therein). Also the question of spectra and dynamics of nonrigid molecules and clusters has been tackled successfully by formulating global potential hypersurfaces and carrying out full dimensional variational quantum dynamical calculations including tunneling processes for up to four-atom systems such as the dimer $(HF)_2$ of hydrogen fluoride[23−26] and also the hydrogen peroxide molecule (HOOH) with the possibility of picosecond stereomutation tunneling.[27−29]

Another important example in the development of our understanding of relating spectra, dynamics, and potential hypersurfaces is the organic prototype molecule methane. Here, it was recognized in the 1980s that, for instance, the effective Hamiltonian anharmonic Fermi resonance coupling constant k_{sbb} (30 cm^{-1}) differed from the corresponding potential constant C_{sbb} (150 cm^{-1}) by about a factor of 5, when properly relating potentials and spectra with vibrational variational calculations on accurate potential hypersurfaces (MRD-CI and beyond),[30−34] although from simple perturbation theory they would be equal. While the early variational calculations for methane were still of reduced dimensionality, today fully 9-dimensional vibrational variational calculations on global potential hypersurfaces for CH_4 can be considered to be the frontier of such research.[35−45]

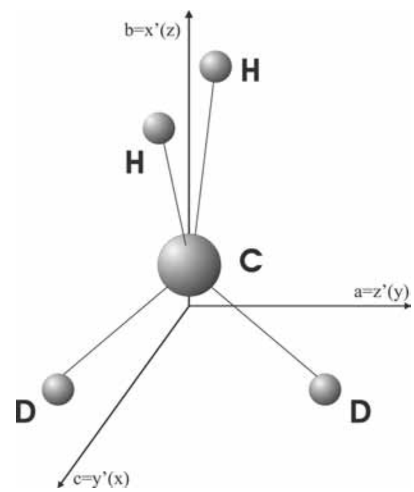

Figure 1. Axes definitions used in the present work for dideuteromethane (CH_2D_2). The unprimed symbols refer to the axis definitions for the C_{2v} symmetry group used in the classification of the vibrational modes. The primed symbols refer to the Cartesian axis definitions of the I^r representation of Watson's *A*-reduced effective Hamiltonian.

In this context, but also because of the importance of methane in many fields of science ranging from reactions kinetics and combustion science to geology, from environmental and planetary science to astrophysics, we have initiated some time ago a detailed study of rovibrational spectra of the methane isotopomer CH_2D_2 with the goal of obtaining an as complete understanding of its vibrational dynamics as possible.[46,47] CH_2D_2 (Figure 1) is particularly suited for a study of its rovibrational dynamics, as it is the

† Part of the "Max Wolfsberg Festschrift".

* Corresponding author. ETH Zürich, Laboratorium für Physikalische Chemie, Wolfgang-Pauli-Strasse 10, CH-8093 Zürich, Switzerland. Phone: +41-44-632 44 22. Fax: +41-44-633 15 98. E-mail: martin@quack.ch.
‡ ETH Zürich.
§ Tomsk State University.
|| Technische Universität Braunschweig.

10.1021/jp809839t CCC: $40.75 © 2009 American Chemical Society
Published on Web 03/05/2009

TABLE 1: Values of the Fundamental Band Centers of CH_2D_2 (in cm^{-1})[a]

ν	Γ^b	ν_0^{exp}/cm^{-1}	ref	assignment[b]
ν_1	A_1	2975.4823	[this work]	CH_2 s-stretching
ν_2	A_1	2203.2171	46, 47, 60	CD_2 s-stretching
ν_3	A_1	1435.1346	46, 47, 59	CH_2 scissoring
ν_4	A_1	1033.0534	46, 47, 59	CD_2 scissoring
ν_5	A_2	1331.4087	46, 47	CH_2 twisting
ν_6	B_1	3012.2595	[this work]	CH_2 a-stretching
ν_7	B_1	1091.185	46, 47, 59	CH_2 rocking
ν_8	B_2	2234.6923	46, 47, 60	CD_2 a-stretching
ν_9	B_2	1236.2771	46, 47, 59	CH_2 wagging

[a] See also ref 47 and references cited therein. [b] s for symmetric, a for antisymmetric, Γ gives the species of the mode in the point group C_{2v}(see Figure 1).

only nonradioactive asymmetric top isotopomer of methane, where the lowered symmetry places fewer restrictions on the electric dipole transitions and removes complications from degenerate vibrational modes as compared to the more highly symmetric isotopomers of C_{3v} and T_d symmetry.

There exists, of course, a substantial body of spectroscopic work on CH_2D_2. Table 1 summarizes the nine vibrational fundamentals as known today. A total of 22 vibrational bands had been studied at moderate to high resolution prior to the present work, where we reanalyze also three of the previously known bands.[48−60] The far-infrared pure rotational spectrum has also been studied with the main goal of deriving the permanent dipole moment of CH_2D_2 including the answer to the long standing question of its sign.[61,62]

In our two previous papers, we have complemented the low-energy spectra by observing and analyzing previously undetected, weak, or forbidden transitions for example to levels of A_2 symmetry or weaker overtone and combinations levels.[46,47] The goal of the present investigation is to very substantially increase our knowledge of the vibrational spectra and dynamics of CH_2D_2 to energies extending beyond $E/hc = 6000\ cm^{-1}$. To achieve such a goal, one may distinguish two strategies. The first one would be to systematically study with stepwise increasing energy all the interacting rovibrational polyads or band systems by means of a complete rovibrational analysis of all observable rovibrational transitions up to a given energy. This is an enormous task, which for the parent isotopomer CH_4 has recently been completed just to the octad[63] (i.e., all levels up to about 4600 cm^{-1}) and for $^{13}CH_4$ up to the pentad[64] (i.e., 3100 cm^{-1}), the octad analysis still being in progress but near to completion. Such complete analyses by necessity can progress only slowly to higher levels of excitation.

A second strategy consists of using spectra taken at low temperatures, which allow for a partial analysis and assignment of spectral lines just for low angular momentum quantum numbers and in particular an assignment and precise measurement of spectral lines belonging to transitions to the $J = 0$ rotational level of the excited vibrational state considered. In this way, one obtains a precise experimental result for the pure vibrational energy for the state considered. For example, this strategy using supersonic jet cavity ring down spectroscopy has been successful in precisely locating the $(\nu_2 + 2\nu_3)$ level of the icosad of CH_4 at 7510.3378 cm^{-1}, far beyond the range accessible to analysis by the first strategy.[65,66] One might also note that even the complete rovibrational analyses of the first strategy, when using room temperature spectra, sometimes cannot directly assign the $J = 0$ levels, if only lines corresponding to higher rotational quantum numbers are accessible by such spectra. Thus the vibrational band centers derived from such analyses frequently do not include a direct observation of the pure vibrational energy, even though an accurate and complete analysis in general can be relied on in providing also the pure vibrational energy correctly.

We shall discuss and illustrate the power of the present second strategy in assigning vibrational levels directly in the following sections. Indeed, we have been able to accurately locate about 70 additional vibrational level positions beyond the ones (22) previously known from many years of research. Figure 2 gives an overview of the number of assigned vibrational levels compared to the total number of expected levels. We shall discuss also the implications of these new results for our understanding of the vibrational dynamics and potential hypersurfaces of methane in the last section of our paper.

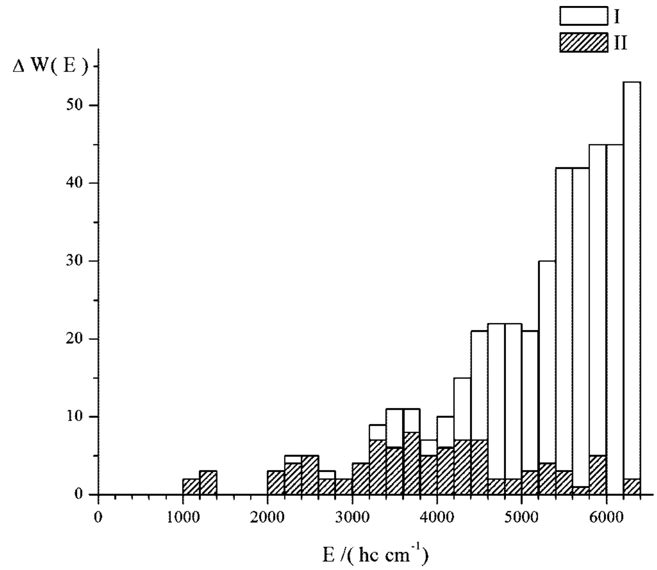

Figure 2. Diagram of the "density" of "cold" (0 K) vibrational bands of the CH_2D_2 molecule in the region below 6500 cm^{-1} (equivalent to the density of levels, i.e., including "forbidden" bands). The diagram shows the number $\Delta W(E_i)$ of levels in intervals i of 200 cm^{-1} for each interval from 0 to 6400 cm^{-1}. The sum $\sum_{i=0}^{N(E)} \Delta W(E_i)$ is the total number of levels $W(E)$ below E. I - total number of possible bands (calculated from the data in Table 6). II - number of bands assigned up to now from experimental spectra (see Table 5).

2. Experimental

The Fourier transform infrared (FTIR) spectrum of CH_2D_2 has been recorded in the wavenumber range from 2800 to 6600 cm^{-1} with the Zürich FTIR spectrometer Bruker IFS 125 prototype 2001.[67,68] The nominal instrumental resolution, defined by 1/MOPD (maximum optical path difference) ranged from 0.0027 to 0.0048 cm^{-1} resulting in essentially Doppler limited spectra. The Doppler widths at 78 K range from about 0.004 cm^{-1} at 2800 cm^{-1} to 0.0096 cm^{-1} at 6600 cm^{-1}. About 100 spectra were typically coadded in each spectral region. A newly built enclosive flow cooling cell based on White optics and embedded in a Dewar was used for recording the cold spectra[69] similar to the design described in refs 70−72. The cooling cell was connected via an evacuated transfer optics chamber to the external parallel port of our spectrometer.[69] It was used here in the static mode (without permanent flow). Optical path lengths ranging from 5 to 10 m were used for the measurements. More details of the experimental setup and procedures can be found in ref 69. A preliminary report of the present work has already been provided in ref 73.

Most of the CH_2D_2 spectra were taken at 78 K. The total sample pressure of a mixture of CH_2D_2 and He in the cell ranged from 2.8 to 3.5 mbar in most cases. In addition, spectra with a pressure of 0.5 mbar were recorded to measure the strong lines without saturation. Pressure broadening can be neglected under these conditions. All spectra were self-apodized. The aperture used was 1 mm. Table 2 summarizes the experimental parameters. The spectra were calibrated with OCS at room temperature (2900 to 3600 cm^{-1})[74] and with $^{12}CH_4$ from 3000 to 6000 cm^{-1}.[75] The CH_2D_2 sample was purchased from Cambridge

TABLE 2: Experimental Setup for the Regions 2800−6600 cm^{-1} of the Infrared Spectrum of CH_2D_2

region/ cm^{-1}	resolution/ cm^{-1}	windows	source	detector	beamsplitter	opt. filter/ cm^{-1}	aperture/ mm	ν_{mirror}/ (kHz)	electr. filter/ cm^{-1}	calib. gas
2800−3700	0.0027	KBr	Globar	InSb	CaF_2	3000−3600	1.0	40	2370−3950	OCS[74]
3200−4600	0.0033	KBr	Tungsten	InSb	CaF_2	3350−4450	1.0	40	2765−5529	CH_4[75]
4200−5600	0.0040	KBr	Tungsten	InSb	CaF_2	4350−5500	1.0	40	2765−7109	CH_4[75]
5200−6400	0.0047	KBr	Tungsten	InSb	CaF_2	5350−6350	1.0	42	3950−7109	CH_4[75]

Isotope Laboratories. The identity, chemical, and isotopic purity (specified to be better than 98%) were obvious from the spectra.

The relative wavenumber accuracy of nonblended, unsaturated, and not too weak lines (about 8500 assignments) can be estimated to be better than 10^{-6} cm^{-1} in the range from 2800 to 6600 cm^{-1}. The absolute wavenumber accuracy depends upon the accuracy of the reference lines used for calibration, which have an uncertainty of about 10^{-4} cm^{-1} for the lower wavenumber range and between 10^{-4} and 10^{-3} cm^{-1} for the higher wavenumber range extending beyond 6000 cm^{-1}.

3. Analysis of the Experimental Spectrum

Figure 3 shows an overview of the experimental FTIR spectrum. As shown above in Figure 2, the density of possible vibrational bands is rapidly increasing with increasing energy. The spectrum is characterized by some strong bands corresponding to first overtone and simple binary combination bands (the total number of this kind of bands allowed in absorption is 37) and further much weaker second overtone and more complex combination bands corresponding to triple excitations (the total number of such infrared bands is 127). The bands which correspond to excitations with four and more vibrational quanta are extremely weak and were not visible in the spectra, as a rule. However, because of some strong resonance interactions even weak third overtone and more complex combination bands can sometimes be identified in the experimental spectrum. In any case, the experimental conditions described in Section 2 allowed us to newly assign 71 vibrational bands which one can compare with the smaller number, 22, of bands studied with high resolution in all previous work together. Transitions with quantum number $J \leq 8$ to 12 for the strong bands and $J \leq 5$ to 6 for the weak bands were assigned in the spectra recorded at a temperature of 78 K.

Figure 4 illustrates the great simplification and improvement of the spectral data obtained in the cold cell at 78 K (upper part) compared to the room temperature spectrum (lower part) in the small spectral range shown around 4441 cm^{-1}. At room temperature, one finds many overlapping, blended, and also weak lines. By contrast, in the cold cell spectrum, the lines are well separated and sharp because of the smaller Doppler widths, often with excellent signal-to-noise ratio, about 500:1 for strong lines and 3:1 for the weakest lines. As discussed in the Introduction, the cold cell spectra allowed us to considerably simplify the assignment of spectra and the identification of pure vibrational level energies. This is illustrated by the level scheme in Figure 5, which shows the ground-state level, the excited rotational levels of the vibrational ground-state with $J'' = 1$, and the possible combinations of K''_a and K''_c. These rotational levels form the possible lower levels for selectively assigned transitions connecting to a rotationless upper vibrational level.

In the case when the upper vibrational state is of A_1-symmetry, one has $K''_a = K''_c = 1$. Analogously, $K''_a = 0$, $K''_c = 1$ applies when the upper vibrational state has the symmetry B_2 or $K''_a = 1$, $K''_c = 0$ for B_1 upper level symmetry. The transition to an upper vibrational level of A_2 symmetry species is forbidden, and such levels have to be measured by other means.[46,47] It should be mentioned that while all the other upper rovibrational levels of a vibrational level are reached by more than one transition, and thus the identities can be confirmed by the corresponding combination differences, the $E_{[J'=0, K'_a=0, K'_c=0]}$ upper rovibrational level (and as a consequence, the "experimental" value of the band center, as well) can be obtained from only one transition as indicated in Figure 5. Therefore, the problem of a correct search for this selected transition in the experimental spectrum is important. This was done in the following way: Fits of the sets of energies of the type $E_{[J', K'_a=0, K'_c=J']}$ ($J' = 1, 2, 3, 4,...$) have been carried out for all bands studied. This allowed us to predict the position of the $[J' = 0,\ K'_a = 0,\ K'_c = 0](v') \leftarrow [J'' = 1,\ K''_a,\ K''_c]\ (v'')$ transition with an accuracy of about 0.01−0.06 cm^{-1}. This accuracy is sufficient to identify beyond doubt the corresponding line in our experimental spectrum.

To illustrate this procedure, Table 3 presents the predicted line positions for the transitions $[J' = 0,\ K'_a = 0,\ K'_c = 0](v') \leftarrow [J'' = 1,\ K''_a, K''_c](v'' = 0)$, in comparison with the experimental line positions for 10 of the lower wavenumber bands analyzed. The matching leaves no room for ambiguity. As an additional confirmation of the correctness of this assignment procedure, the "smooth" behavior of the line strengths in the sets of transitions $[J', K'_a = 0, K'_c = J'](v') \leftarrow [J'' = J' + 1, K''_a = 0/1, K''_c = J' + 1/J'](v'' = 0)$ can be mentioned. Figure 6a, 6b, and 6c give an illustration of the procedure for three bands of different symmetry. One can see very nicely the various assigned transitions of the bands and the convergence to the predicted selected lines marked by the arrows. These lines provide thus the transitions to the rotationless upper vibrational levels, and by adding the rotational energies of the lower level of the transition one obtains as indicated in Table 3 finally the upper vibrational energy E'_{vib}.

The lower level rotational energies in Figure 5 cannot be obtained from the pure rotational transitions or from simple combination differences, as the corresponding transitions are forbidden by symmetry in C_{2v}. However, we have reanalyzed numerous ground-state combination differences in terms of rotational energies for low J levels and derived the relevant $J = 1$ level energies in Figure 5 from the appropriate fit of effective rotational Hamiltonian constants to the spectral data. This extrapolation to $J = 1$ level energies provides the data for E''_{rot} in Table 3 with an accuracy of at least five significant digits. Therefore, the remaining uncertainty does not affect the upper vibrational level energies determined by adding the transition energy to the lower level rotational energy. Table 4 gives the corresponding rotational parameters.

In total, more than 8500 rovibrational transitions were assigned to 71 excited vibrational levels. More than 8400 of these transitions were confirmed by combination differences. The list of experimental band centers is given in Table 5 together with all calculated levels as described in Section 4 in detail. When four digits after the decimal point are given for the experimental result, then the band center was derived directly by the procedure described above. These data should have an uncertainty limited only by the calibration and peak finding uncertainties, which are in the range between 0.0001 and 0.001 cm^{-1} (see Section 2). The complete listing of all assigned rovibrational transitions will be reported in conjunction with a partially complete rovibrational analysis including interactions for high J levels.[76]

In a few cases, we were able to estimate the band center only by a less accurate fit procedure. For these four levels, we give only one digit after the decimal point, and we did not use those data in

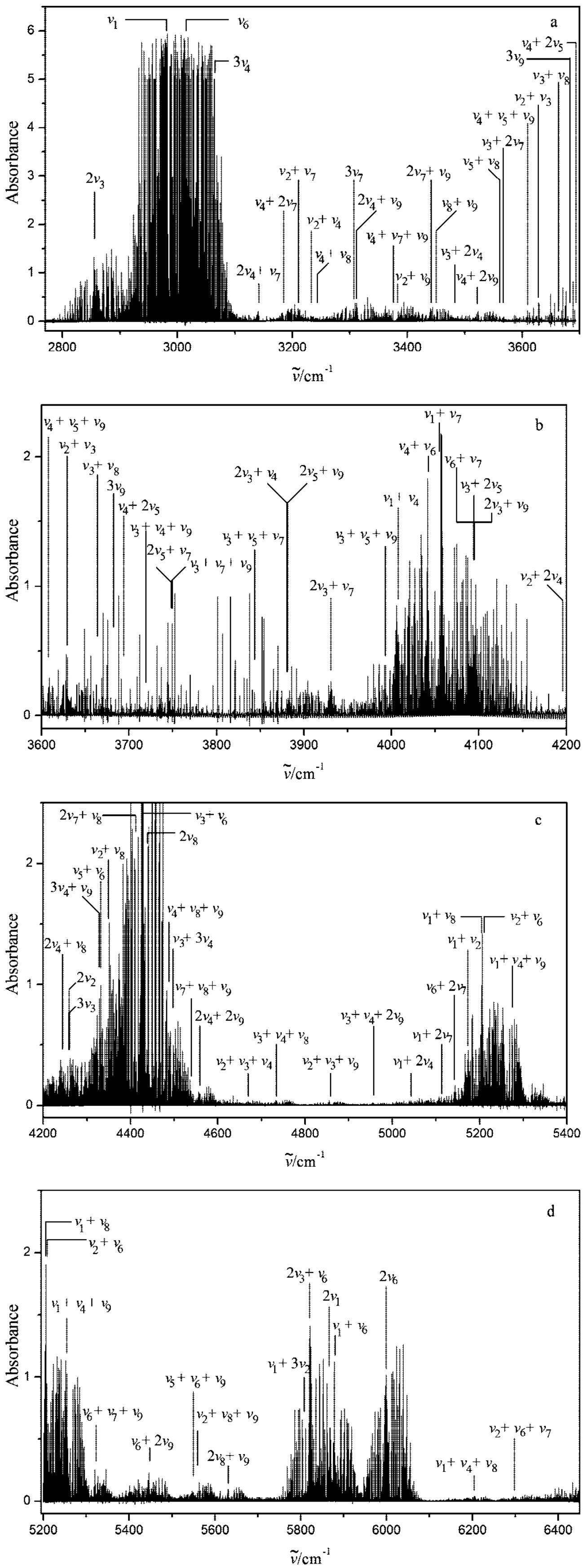

Figure 3. Survey spectrum of CH_2D_2 in the region of 2800−6500 cm^{-1}. Experimental conditions are presented in Table 1. The parts a, b, c, d cover the range from 2800 to 6400 cm^{-1}. The decadic absorbance lg(I_0/I) is given on the ordinate.

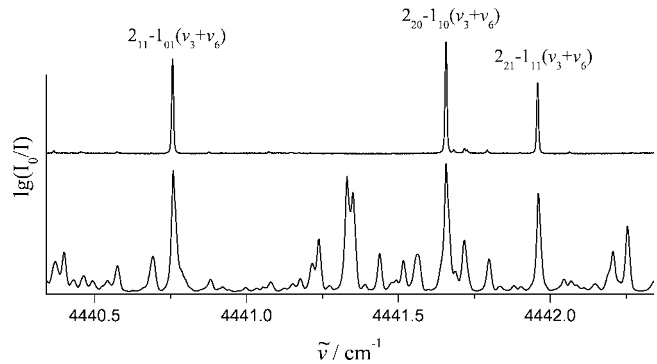

Figure 4. Small portion of the spectrum of the CH_2D_2 molecule in the region of the $\nu_3 + \nu_6$ band. Upper trace: Bruker IFS 125 prototype (ZP 2001) spectrum at 78 K. Lower trace: Bomem DA002 spectrum at 293 K. Both spectra are essentially Doppler limited.

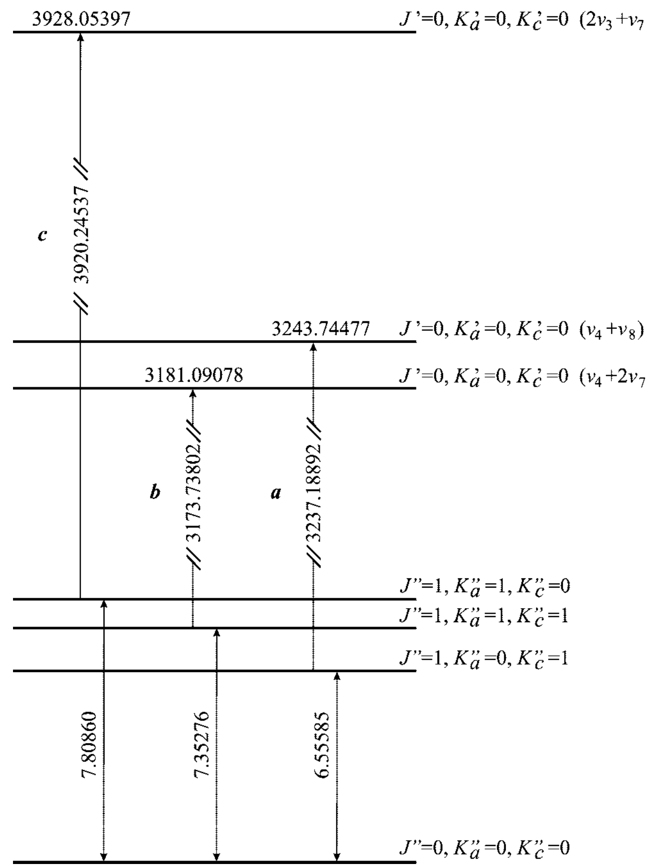

Figure 5. Level scheme explaining the procedure to derive the ($J' =$ 0, v') level energy for an excited level v' from experimental transition wavenumbers and ground-state rotational energies. All transition wavenumbers and term values are given in cm^{-1}. *a* stands for *a*-type transition, *b* for *b*-type, *c* for *c*-type.

the final fits of data as we cannot specify a definitive uncertainty estimate. These four band centers refer to the $\nu_4 + \nu_7 + \nu_9$, $\nu_3 + \nu_7 + \nu_9$, $\nu_5 + \nu_6$, and $\nu_5 + \nu_8$ bands. The first two correspond to transitions where the upper vibrational state is of A_2 symmetry, and as a consequence, they are "forbidden" in absorption. They appear in the spectrum only for $J > 0$ because of strong resonance interactions with neighboring states showing allowed infrared transitions. This circumstance leads to the absence of the transition to the [$J' = 0$, $K_a' = 0$, $K_c' = 0$] upper rovibrational state. Thus, the corresponding band centers cannot be derived from the experimental data and can only be obtained from the fit. Furthermore, also in the cases of the $\nu_5 + \nu_6$ and $\nu_5 + \nu_8$ bands, which are allowed, but very weak, the P-type transitions [$J' = 0$, $K_a' =$

TABLE 3: Line Positions and Levels for the Transitions [$J' = 0, K_a' = 0, K_c' = 0$]($v'$) ← [$J'' = 1, K_a'', K_c''$]($v'' = 0$) for Some Absorption Bands of CH_2D_2 (in cm^{-1})

band	$(0 \leftarrow 1)^{\text{predict.}}$	$(0 \leftarrow 1)^{\text{exp.}}$	$J''\ K_a''\ K_c''$	$E''_{\text{rot.}}/hc$	$E'_{\text{vib.}}/hc$
$2\nu_3$ (A_1)	2848.315	2848.3122	1 1 1	7.3528	2855.6650
ν_1 (A_1)	2968.130	2968.1295	1 1 1	7.3528	2975.4823
ν_6 (B_1)	3004.450	3004.4509	1 1 0	7.8086	3012.2595
$3\nu_4$ (A_1)	3058.782	3058.7813	1 1 1	7.3528	3066.1341
$2\nu_4 + \nu_7$ (B_1)	3133.876	3133.8177	1 1 0	7.8086	3141.6263
$\nu_4 + 2\nu_7$ (A_1)	3173.783	3173.7380	1 1 1	7.3528	3181.0908
$\nu_2 + \nu_7$ (B_1)	3202.457	3202.4589	1 1 0	7.8086	3210.2675
$\nu_2 + \nu_4$ (A_1)	3226.329	3226.3281	1 1 1	7.3528	3233.6809
$\nu_4 + \nu_8$ (B_2)	3237.187	3237.1889	1 0 1	6.5559	3243.7448
$3\nu_7$ (B_1)	3298.956	3298.9560	1 1 0	7.8086	3306.7646

0, $K_c' = 0$](v') ← [$J'' = 1$, K_a'', K_c'']($v'' = 0$) could not be identified beyond doubt in the spectrum. Therefore, the centers of the $\nu_5 + \nu_6$ and $\nu_5 + \nu_8$ bands were also not derived from an experimental transition but were estimated from the fit.

The level assignment in the first column of Table 5, given in terms of the excitation of the normal modes, has, of course, limited significance when there is extensive state mixing particularly at higher excitations. The symmetry assignment in C_{2v} (see Figure 1) is, however, robust.

One can see from Table 5 that below about 4500 cm^{-1} the large majority of vibrational levels could actually be observed, whereas the fraction of experimentally assigned levels rapidly decreases above 4500 cm^{-1}, many bands being too weak for detection under our conditions (see also Figure 2).

The predictions derived in the following section and summarized in Table 5 as well might help to assign further levels in spectra taken under appropriate conditions.

4. Theoretical Background, Symmetry, Hamiltonian Model, and Vibrational Assignment

CH_2D_2 is an asymmetric top molecule with C_{2v} point group symmetry (see Figure 1). Its nine vibrational modes q_K have the symmetry species as given for the corresponding fundamentals in Table 1. Similarly, the vibrational wave functions (v_1, v_2, v_3, v_4, v_5, v_6, v_7, v_8, v_9), where the symbol v_i denotes the number of quanta in the i-th vibrational mode, belong to one of the four symmetry species A_1, A_2, B_1, or B_2.The complete permutation inversion group for CH_2D_2 is $S^*_{2,2}$ of order 8;[77,78] however, tunneling is not observed due to the high barrier,[79] and the induced representation $\Gamma(MS_4 \sim C_{2v}) \uparrow \Gamma(S^*_{2,2})$ indicates that both positive and negative parities arise for all sublevels in contrast to CH_4 and CH_3D. More details of symmetry and nuclear spin statistics are discussed in refs 76 and 80.

As shown in Figure 2, one expects a rapid increase of the density of vibrational states with increasing wavenumber. Furthermore, the infrared spectrum is complicated by the presence of numerous and strong resonance interactions between many vibrational states. As a consequence, even a preliminary analysis of the infrared spectra of the CH_2D_2 molecule requires consideration of the relevant resonance interactions both of the Fermi and Darling−Dennison as well as of the Coriolis types. In accordance with the general symmetry properties, such Hamiltonians have the following form[4−11,47,59]

$$H^{v.-r.} = \sum_{v,\tilde{v}} |v\rangle\langle\tilde{v}| H_{v\tilde{v}} \tag{1}$$

where the summation extends over all interacting vibrational states. The diagonal operators H_{vv} describe unperturbed rotational structures of the vibrational states involved. The nondiagonal operators $H_{v\tilde{v}}$, ($v \neq \tilde{v}$) describe different kinds of resonance interactions between the states $|v\rangle$ and $|\tilde{v}\rangle$. The diagonal block operators have the same form for all the vibrational states involved (they are so-called Watson Hamiltonians, here in the A-reduction and I^r representation[81,82])

$$H_{vv} = E^v + \left[A^v - \frac{1}{2}(B^v + C^v)\right]J_z^2 + \frac{1}{2}(B^v + C^v)J^2 + \frac{1}{2}(B^v - C^v)J_{xy}^2 - \Delta_K^v J_z^4 - \Delta_{JK}^v J_z^2 J^2 - \Delta_J^v J^4 - \delta_K^v[J_z^2, J_{xy}^2] - 2\delta_J^v J^2 J_{xy}^2 + \ldots \tag{2}$$

where J_α ($\alpha = x, y, z$) are the components of the angular momentum operator defined in the molecule-fixed coordinate system; $J_{xy}^2 = J_x^2 - J_y^2$; A^v, B^v, and C^v are the effective rotational constants connected with the vibrational states v; and the other parameters are the different centrifugal distortion coefficients.

We can distinguish between four types of coupling operators $H_{v\tilde{v}}$ ($v \neq \tilde{v}$) corresponding to the four different types of resonance interactions which can occur in C_{2v} asymmetric top molecules. If the product $\Gamma = \Gamma^v \otimes \Gamma^{\tilde{v}}$ of the symmetry species of the states v and $\tilde{v}$ is equal to A_1 (i.e., $\Gamma^v = \Gamma^{\tilde{v}}$), then the states v and $\tilde{v}$ are connected by an anharmonic resonance interaction, and the corresponding interaction operator has the form

$$H_{v\tilde{v}} = {}^{v\tilde{v}}F_0 + {}^{v\tilde{v}}F_K J_z^2 + {}^{v\tilde{v}}F_J J^2 + \ldots + {}^{v\tilde{v}}F_{xy}(J_x^2 - J_y^2) + \ldots \tag{3}$$

If the product is $\Gamma = B_1$, then the states v and $\tilde{v}$ are connected by a Coriolis resonance interaction of the form

$$H_{v\tilde{v}} = iJ_z H_{v\tilde{v}}^{(1)} + \{J_x, J_y\}_+ H_{v\tilde{v}}^{(2)} + H_{v\tilde{v}}^{(2)}\{J_x, J_y\}_+ + \ldots \tag{4}$$

When $\Gamma = B_2$, the following Coriolis interaction is allowed

$$H_{v\tilde{v}} = iJ_y H_{v\tilde{v}}^{(1)} + H_{v\tilde{v}}^{(1)} iJ_y + \{J_x, J_z\}_+ H_{v\tilde{v}}^{(2)} + H_{v\tilde{v}}^{(2)}\{J_x, J_z\}_+ + \ldots \tag{5}$$

Finally, when $\Gamma = A_2$, a Coriolis interaction of the following type is possible

$$H_{v\tilde{v}} = iJ_x H_{v\tilde{v}}^{(1)} + H_{v\tilde{v}}^{(1)} iJ_x + \{J_y, J_z\}_+ H_{v\tilde{v}}^{(2)} + H_{v\tilde{v}}^{(2)}\{J_y, J_z\}_+ \ldots \tag{6}$$

The operators $H_{v\tilde{v}}^{(i)}$, $i = 1, 2, 3, \ldots$ in eqs 4−6 have the form

$$H_{v\tilde{v}}^{(i)} = \frac{1}{2}{}^{v\tilde{v}}C^i + {}^{v\tilde{v}}C_K^i J_z^2 + \frac{1}{2}{}^{v\tilde{v}}C_J^i J^2 + \ldots \tag{7}$$

These equations are used in the rovibrational analysis, which was necessary in the assignment procedure.

The information derived from the rovibrational analysis providing effective Hamiltonian parameters can be considered to be the first step toward the determination of an empirical multidimensional potential hypersurface of methane. The small experimental uncertainty (estimated to be between 0.0001 and 0.001 cm^{-1} for different bands and different spectral regions and always below 0.01 cm^{-1}) of the numerous band centers allowed us to correctly determine the values of the harmonic wavenumbers ω_k, anharmonic coefficients x_{kj}, and of some resonance interaction parameters. A total of 74 band centers derived in the present contribution (71 new and 3 redetermined for the bands $2\nu_3$, ν_1, and ν_6) were added to the 19 band centers known previously from refs 46, 47, 57, 59, and 60and fitted with the simple model of a vibrational Hamiltonian matrix which takes into account some relevant resonance interactions

$$H^{v.} = \sum_{v,\tilde{v}} |v\rangle\langle\tilde{v}| h_{v\tilde{v}} \tag{8}$$

Here the summation includes all vibrational states studied. The diagonal elements of the matrix have the form

$$h_{vv} = \sum_k \omega_k\left(v_k + \frac{1}{2}\right) + \sum_{k,m\geq k} x_{km}\left(v_k + \frac{1}{2}\right)\left(v_m + \frac{1}{2}\right) + \sum_{k,m\geq k,n\geq m} y_{kmn}\left(v_k + \frac{1}{2}\right)\left(v_m + \frac{1}{2}\right)\left(v_n + \frac{1}{2}\right) \tag{9}$$

Concerning resonance interaction matrix elements, it was found that the following types are important for the current

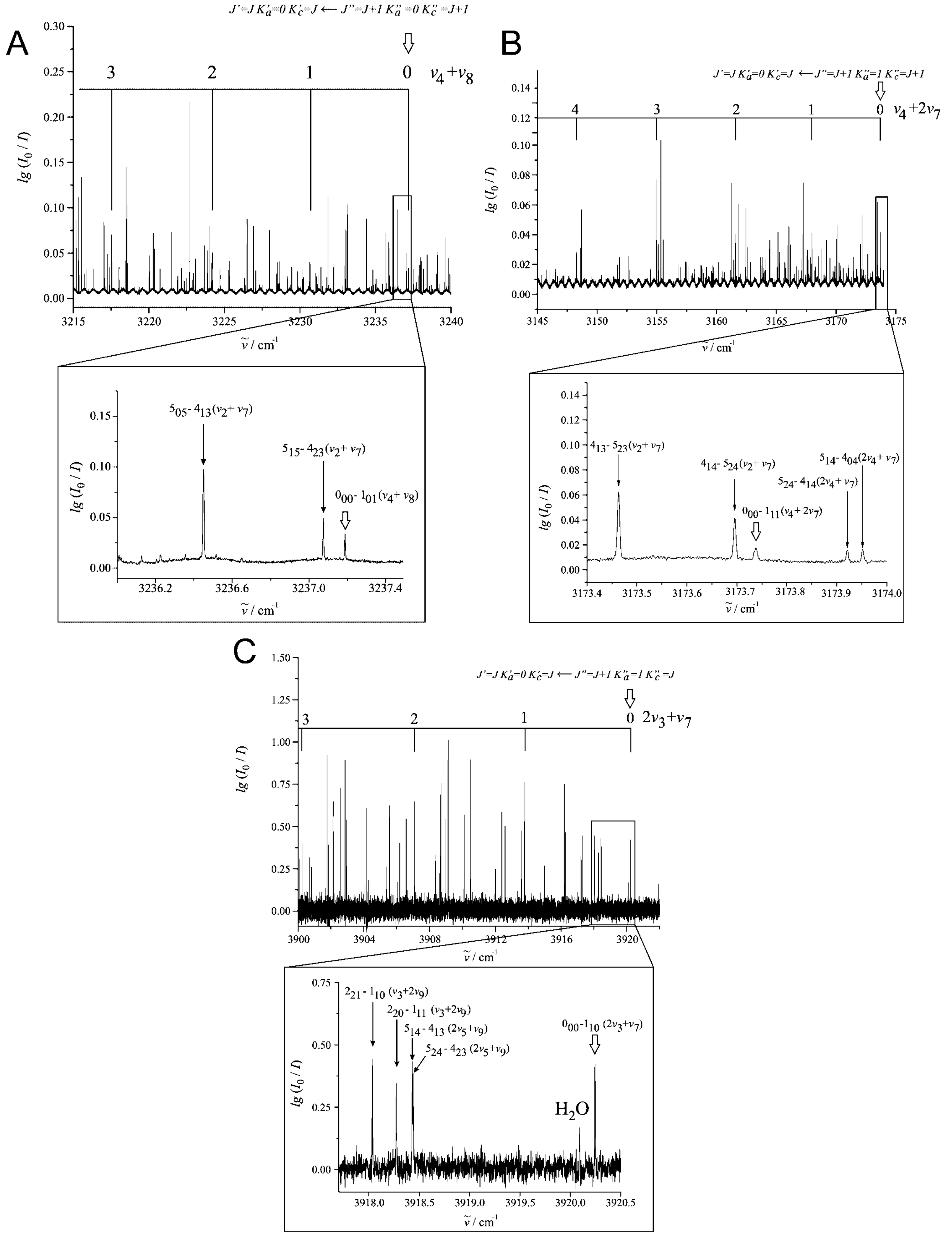

Figure 6. Set of transitions $[J', K_a' = 0, K_c' = J'](v') \leftarrow [J'' = J' + 1, K_a'' = 0/1, K_c'' = J' + 1/J'](v'' = 0)$ for the bands of different symmetry: (a) *a*-type transitions for the B_2-symmetry upper vibrational state (the lower is the ground vibrational state of the A_1-symmetry); (b) *b*-type transitions for the A_1-symmetry upper state; (c) *c*-type transitions for the B_1-symmetry upper state. The first line of progressions, which corresponds the transitions with $J' = 0$, can be recognized beyond doubt. Alternation of the stronger and weaker lines in the set is caused by the nuclear spin statistic of rotational levels. The lower parts of the Figures 6a−6c show in more detail the sections of the spectra close to the transition $[J' = 0, K_a' = 0, K_c' = 0](v') \leftarrow [J'' = 1, K_a'' = 0/1, K_c'' = 1/0](v'')$. Assigned lines of some other bands also indicated.

TABLE 4: Ground State Rotational Parameters (in cm^{-1}) for CH_2D_2 Obtained from Ground-State Combination Differences (GSCD) of the Present Study

parameter	present study	from ref 47
1	2	3
A	4.3028927(25)[c]	4.3028950
B	3.5059459(24)	3.5059379
C	3.0500947(22)	3.0500936
$\Delta_K/10^{-4}$	0.74406(150)	0.741677
$\Delta_{JK}/10^{-4}$	−0.15861(147)	−0.153933
$\Delta_J/10^{-4}$	0.470106(405)	0.468558
$\delta_K/10^{-4}$	−0.15729(167)	−0.158331
$\delta_J/10^{-4}$	0.090279(252)	0.089864
$H_K/10^{-8}$	−0.104214[b]	−0.104214
$H_{KJ}/10^{-8}$	0.94465[b]	0.94465
$H_{JK}/10^{-8}$	−0.34124[b]	−0.34124
$H_J/10^{-8}$	0.181618[b]	0.181618
$h_K/10^{-8}$	0.34986[b]	0.34986
$h_{JK}/10^{-8}$	−0.25873[b]	−0.25873
$h_J/10^{-8}$	0.069674[b]	0.069674
N[a]	134	134
n[a]	8	
d_{rms}	0.000066	0.000071

[a] Here N is the number of GSCD used in the fit; n is the number of varied parameters. [b] Constrained to the value from column 3. [c] Uncertainties are given in parentheses in terms of one standard deviation in units of the last digits given.

problem and should be taken into account in defining the parameters of the effective Hamiltonian to be reported below.

1. (first type)

$$h_{v\tilde{v}} = \frac{\gamma_{3499}}{8}(2v_3 \pm 1 + 1)^{1/2}(2v_4 \pm 1 + 1)^{1/2}(v_9 \mp 1 + 1)^{1/2}(v_9 \mp 1)^{1/2} \quad (10)$$

if $|v\rangle = (..., v_3, v_4,..., v_9)$ and $|\tilde{v}\rangle = (..., v_3 \pm 1, v_4 \pm 1,..., v_9 \mp 2)$;

2. (second type)

$$h_{v\tilde{v}} = \frac{1}{4}(2v_2 \pm 1 + 1)^{1/2}(v_7 \mp 1 + 1)^{1/2}(v_7 \mp 1)^{1/2}(k_{277} + \delta_{277}(2v_7 \mp 2 + 1)) \quad (11)$$

if $|v\rangle = (..., v_2,..., v_7,...)$ and $|\tilde{v}\rangle = (..., v_2 \pm 1,..., v_7 \mp 2,...)$;

3. (third type)

$$h_{v\tilde{v}} = \frac{k_{489}}{8}(2v_8 \pm 1 + 1)^{1/2}(2v_4 \mp 1 + 1)^{1/2}(2v_9 \mp 1 + 1)^{1/2} \quad (12)$$

if $|v\rangle = (..., v_4,..., v_8, v_9)$ and $|\tilde{v}\rangle = (..., v_4 \mp 1,..., v_8 \pm 1, v_9 \mp 1)$;

4. (fourth type)

$$h_{v\tilde{v}} = \frac{k_{133}}{4}(2v_1 \pm 1 + 1)^{1/2}(v_3 \mp 1 + 1)^{1/2}(v_3 \mp 1)^{1/2} \quad (13)$$

if $|v\rangle = (v_1,..., v_3,...)$ and $|\tilde{v}\rangle = (v_1 \pm 1,..., v_3 \mp 2,...)$;

5. (fifth type)

$$h_{v\tilde{v}} = \frac{\gamma_{3759}}{16}(2v_3 \pm 1 + 1)^{1/2}(2v_7 \pm 1 + 1)^{1/2}(2v_5 \mp 1 + 1)^{1/2}(2v_9 \mp 1 + 1)^{1/2} \quad (14)$$

if $|v\rangle = (..., v_3,..., v_5,..., v_7,..., v_9)$ and $|\tilde{v}\rangle = (..., v_3 \pm 1,..., v_5 \mp 2,..., v_7 \pm 1,..., v_9 \mp 1)$;

6. (sixth type)

$$h_{v\tilde{v}} = \frac{\gamma_{1166}}{4}(v_1 \pm 1 + 1)^{1/2}(v_1 \pm 1)^{1/2}(v_6 \mp 1 + 1)^{1/2}(v_6 \mp 1)^{1/2} \quad (15)$$

if $|v\rangle = (v_1,..., v_6,...)$ and $|\tilde{v}\rangle = (v_1 \pm 2,..., v_6 \mp 2,...)$.

Those quantum numbers v_i, which are not mentioned in eqs 10−15, have the same values in both of the states $|v\rangle$ and $|\tilde{v}\rangle$.

5. Results of the Final Analysis and Discussion

In the final calculation, a set of 47 parameters were adjusted in a least-squares analysis. The values obtained are presented in columns 2 of Tables 6 and 7 together with their statistical confidence intervals (1σ). The parameters reproduce the experimental values of the band centers used in the fit with a root-mean-square deviation $d_{rms} = 0.67$ cm^{-1}. Columns 3 of Tables 6 and 7 present, for comparison, also the corresponding ab initio data from ref 83. In column 3 of Table 5, the values of the band centers calculated with the parameters from columns 2 of Tables 6 and 7 are listed. There is in general excellent agreement between the experimental and calculated values of the band centers. The root-mean-square deviation of the fit is 0.67 cm^{-1}, with few differences being larger than 1 cm^{-1} and none larger than 2 cm^{-1} for the 89 fitted bands.

Some points are noteworthy in the context of the fit. First, in the fit procedure we did not adjust the harmonic wavenumbers ω_k ($k = 1,..., 9$), but instead we determined the parameters F_{ij} of the harmonic force field as defined by[3,35,84]

$$2V^{(2)} = F_{11}S_1^2 + F_{22}(S_{2a}^2 + S_{2b}^2) + F_{33}(S_{3x}^2 + S_{3y}^2 + S_{3z}^2) + 2F_{34}(S_{3x}S_{4x} + S_{3y}S_{4y} + S_{3z}S_{4z}) + F_{44}(S_{4x}^2 + S_{4y}^2 + S_{4z}^2) \quad (16)$$

for methane, because for a given r_e-structure[46,47] the nine harmonic wavenumbers ω_k are exactly described by the five force constants F_{ij} of eq 16. This smaller set of parameters was thus used in the fit.

Second, some of the x_{kl} and F_{ij} turn out to be unstable in the fit to the set of available experimental band centers. The confidence intervals of some parameters were found to be comparable with or even larger than the absolute values of parameters themselves. These parameters were therefore constrained to the values predicted on the basis of a preliminary estimate of the "experimental" potential energy surface of the methane molecule, refs 80 and 83, and were not fitted. The corresponding values are given in Tables 6 and 7 without confidence intervals.

The centers of the four bands $\nu_4 + \nu_7 + \nu_9$, $\nu_3 + \nu_7 + \nu_9$, $\nu_5 + \nu_6$, and $\nu_5 + \nu_8$ were not included in the fit as discussed above. These values as given in column 3 of Table 5 are thus predictions, showing a good predictive power of the simple model at least for these bands. One can compare also with the band centers predicted using the parameters from the ab initio calculations of ref 83. Here many of the predicted values are quite different from the experimental result and from our model. The discrepancies frequently exceed 20 cm^{-1} and more. When one looks more closely into the details of the discrepancies, one finds that while the CH-stretching fundamentals ν_1 and ν_6 are rather well described by the ab initio theory of 83 the CD-stretching fundamentals ν_2 and ν_8 show discrepancies on the order of 10−20 cm^{-1}. It is thus not surprising that more highly excited levels involving CD-stretching excitations are incorrectly predicted by ab initio theory. The discrepancies do obviously not arise from the harmonic force field, as experimental and theoretical harmonic wavenumbers in Table 7 agree well. Indeed, our experimental results for the harmonic frequencies agree much better with the ab initio theory of Lee, Martin, and Taylor[83] than with the experimental result of Gray and Robiette,[85] which for a long time constituted the best experimental result but is now

TABLE 5: Values of the Band Centers of the CH_2D_2 Molecule (in cm^{-1})[a]

band	center[83]	center, calc.	center, exp.	ref
1	2	3	4	5
ν_4, A_1	1033.89	1032.18	1033.053	59
ν_7, B_1	1093.49	1090.33	1091.185	59
ν_9, B_2	1235.31	1236.87	1236.277	59
ν_5, A_2	1330.73	1331.49	1331.409	47
ν_3, A_1	1435.72	1434.84	1435.135	59
$2\nu_4$, A_1	2058.80	2053.94	2054.163	60
$\nu_4 + \nu_7$, B_1	2128.11	2121.63	2124.678	60
ν_2, A_1	2167.65	2145.76	2145.692	60
$2\nu_7$, A_1	2183.22	2203.39	2203.217	60
ν_8, B_2	2246.64	2235.53	2234.692	60
$\nu_4 + \nu_9$, B_2	2267.29	2285.55	2285.977	60
$\nu_7 + \nu_9$, A_2	2332.39	2329.66	2329.698	47
$\nu_4 + \nu_5$, A_2	2365.13	2365.14		
$\nu_5 + \nu_7$, B_2	2424.60	2422.20	2422.025	46
$2\nu_9$, A_1	2461.92	2459.14	2458.794	46
$\nu_3 + \nu_4$, A_1	2468.09	2469.13	2469.201	46
$\nu_3 + \nu_7$, B_1	2521.70	2515.49	2515.449	46
$\nu_5 + \nu_9$, B_1	2557.29	2561.06	2560.547	46
$2\nu_5$, A_1	2657.04	2657.69	2658.335	57
$\nu_3 + \nu_9$, B_2	2671.70	2671.53	2671.684	57
$\nu_3 + \nu_5$, A_2	2766.02	2766.89		
$2\nu_3$, A_1	2858.01	2855.40	2855.6650	tw
ν_1, A_1	2972.07	2975.51	2975.4823	tw
ν_6, B_1	3008.02	3012.03	3012.2595	tw
$3\nu_4$, A_1	3074.72	3065.29	3066.1341	tw
$2\nu_4 + \nu_7$, B_1	3153.74	3142.53	3141.6263	tw
$\nu_2 + \nu_4$, A_1	3202.39	3182.76	3183.6831	tw
$\nu_2 + \nu_7$, B_1	3253.12	3210.87	3210.2675	tw
$\nu_4 + 2\nu_7$, A_1	3253.13	3234.44	3233.6809	tw
$2\nu_4 + \nu_9$, B_2	3264.92	3243.30	3243.7448	tw
$3\nu_7$, B_1	3269.19	3306.81	3306.7646	tw
$\nu_4 + \nu_8$, B_2	3290.29	3313.54	3313.6709	tw
$\nu_7 + \nu_8$, A_2	3333.13	3320.80		
$\nu_4 + \nu_7 + \nu_9$, A_2	3365.10	3374.53	3375.9[b]	tw
$\nu_2 + \nu_9$, B_2	3398.63	3380.82	3381.4722	tw
$2\nu_4 + \nu_5$, A_2	3390.55	3388.37		
$2\nu_7 + \nu_9$, B_2	3425.71	3439.33	3439.4943	tw
$\nu_4 + 2\nu_9$, A_1	3466.34	3451.08	3449.1771	tw
$\nu_4 + \nu_5 + \nu_7$, B_2	3459.73	3454.98		
$\nu_2 + \nu_5$, A_2	3491.06	3473.85		
$\nu_3 + 2\nu_4$, A_1	3491.46	3484.72	3484.3728	tw
$\nu_8 + \nu_9$, A_1	3491.99	3521.63	3522.1169	tw
$\nu_5 + 2\nu_7$, A_2	3514.72	3531.73		
$\nu_3 + \nu_4 + \nu_7$, B_1	3554.78	3542.35		
$\nu_7 + 2\nu_9$, B_1	3562.59	3558.11		
$\nu_5 + \nu_8$, B_1	3567.72	3562.07	3561.3[b]	tw
$\nu_2 + \nu_3$, A_1	3603.90	3569.23	3569.6894	tw
$\nu_4 + \nu_5 + \nu_9$, B_1	3589.78	3609.36	3609.7748	tw
$\nu_3 + 2\nu_7$, A_1	3601.33	3626.93	3626.6605	tw
$\nu_5 + \nu_7 + \nu_9$, A1	3654.73	3656.33		
$\nu_3 + \nu_8$, B_2	3679.31	3665.11	3663.8061	tw
$3\nu_9$, B_2	3679.82	3679.92	3680.0021	tw
$\nu_4 + 2\nu_5$, A_1	3691.94	3692.80	3692.5422	tw
$\nu_2 + 2\nu_9$, A_1	4620.89	4558.21	4557.8901	tw
$\nu_3 + 2\nu_4 + \nu_7$, B_1	4578.87	4560.06		
$\nu_4 + \nu_5 + 2\nu_7$, A_2	4550.58	4564.18		
$\nu_4 + \nu_5 + \nu_8$, B_1	4586.50	4572.48		
$2\nu_4 + 2\nu_9$, A_1	4513.07	4595.48		
$\nu_3 + \nu_4 + 2\nu_7$, A_1	4637.71	4606.41		
$\nu_4 + \nu_7 + 2\nu_9$, B_1	4593.38	4612.33		
$2\nu_4 + \nu_5 + \nu_9$, B_1	4613.28	4625.58		
$\nu_5 + 3\nu_7$, B_2	4601.08	4635.12		
$\nu_2 + \nu_3 + \nu_7$, B_1	4679.27	4638.63		
$2\nu_7 + 2\nu_9$, A_1	4659.51	4643.77		
$\nu_8 + 2\nu_9$, B_2	4677.33	4655.55		
$\nu_5 + \nu_7 + \nu_8$, A_1	4654.59	4657.08		
$\nu_4 + 3\nu_9$, B_2	4707.97	4676.48		
$\nu_2 + \nu_3 + \nu_4$, A_1	4634.53	4668.22	4668.2418	tw
$\nu_4 + \nu_5 + \nu_7 + \nu_9$, A_1	4687.97	4700.07		
$\nu_3 + 3\nu_7$, B_1	4682.34	4700.74		
$\nu_3 + \nu_4 + \nu_9$, B_2	3702.14	3718.76	3719.5909	tw
$2\nu_5 + \nu_7$, B_1	3751.29	3748.78	3748.3253	tw
$\nu_3 + \nu_7 + \nu_9$, A_2	3761.25	3749.11	3749.0[b]	tw
$\nu_5 + 2\nu_9$, A_2	3775.14	3781.97		
$\nu_3 + \nu_4 + \nu_5$, A_2	3798.88	3798.88		
$\nu_3 + \nu_5 + \nu_7$, B_2	3852.36	3842.95	3842.4298	tw
$2\nu_3 + \nu_4$, A_1	3888.82	3880.88	3881.0299	tw
$2\nu_5 + \nu_9$, B_2	3874.83	3881.55	3882.0088	tw
$\nu_3 + 2\nu_9$, A_1	3898.96	3900.47		
$2\nu_3 + \nu_7$, B_1	3936.44	3928.25	3928.0540	tw
$3\nu_5$, A_2	3978.91	3978.59		
$\nu_3 + \nu_5 + \nu_9$, B_1	3993.23	3995.88	3996.0063	tw
$\nu_1 + \nu_4$, A_1	4003.91	4005.23	4005.6345	tw
$\nu_4 + \nu_6$, B_1	4040.50	4043.07	4042.5767	tw
$\nu_1 + \nu_7$, B_1	4056.77	4057.95	4057.5764	tw
$4\nu_4$, A_1	4081.66	4066.23		
$\nu_6 + \nu_7$, A_1	4090.24	4091.29	4092.0424	tw
$\nu_3 + 2\nu_5$, A_1	4091.88	4091.64		
$2\nu_3 + \nu_9$, B_2	4094.63	4091.90	4091.0094	tw
$3\nu_4 + \nu_7$, B_1	4170.40	4153.01		
$2\nu_3 + \nu_5$, A_2	4187.84	4185.61		
$\nu_2 + 2\nu_4$, A_1	4228.15	4197.33	4197.2292	tw
$\nu_1 + \nu_9$, B_2	4201.24	4211.77		
$\nu_6 + \nu_9$, A_2	4232.52	4236.17		
$\nu_2 + \nu_4 + \nu_7$, B_1	4288.60	4240.96		
$2\nu_4 + \nu_8$, B_2	4274.20	4242.94	4243.9468	tw
$2\nu_4 + 2\nu_7$, A_1	4244.93	4255.09		
$3\nu_3$, A_1	4307.05	4262.77	4263.0639	tw
$2\nu_2$, A_1	4266.81	4263.02	4263.2818	tw
$\nu_1 + \nu_5$, A_2	4291.05	4295.64		
$\nu_2 + \nu_4 + \nu_9$, B_2	4431.45	4328.82	4327.2766	tw
$\nu_4 + \nu_7 + \nu_8$, A_2	4352.13	4328.92		
$\nu_2 + 2\nu_7$, A_1	4334.84	4331.53		
$\nu_5 + \nu_6$, B_2	4325.88	4331.60	4332.0[b]	tw
$\nu_4 + 3\nu_7$, B_1	4305.27	4337.04		
$\nu_2 + \nu_8$, B_2	4354.57	4348.15	4348.1006	tw
$3\nu_4 + \nu_5$, A_2	4407.00	4401.05		
$2\nu_4 + \nu_7 + \nu_9$, A_2	4388.82	4401.57		
$\nu_1 + \nu_3$, A_1	4400.55	4401.81		
$2\nu_7 + \nu_8$, B_2	4415.86	4412.40	4413.7498	tw
$4\nu_7$, A_1	435141	4415.75		
$3\nu_4 + \nu_9$, B_2	4304..29	4423.72		
$\nu_3 + \nu_6$, B_1	4421.61	4425.36	4425.5493	tw
$\nu_4 + \nu_8 + \nu_9$, A_1	4482.70	4435.43	4436.4881	tw
$\nu_2 + \nu_7 + \nu_9$, A_2	4487.69	4449.14		
$2\nu_4 + \nu_5 + \nu_7$, B_2	4485.88	4477.31		
$\nu_4 + 2\nu_7 + \nu_9$, B_2	4459.15	4479.11		
$2\nu_8$, A_1	4456.12	4485.57	4485.2623	tw
$\nu_3 + 3\nu_4$, A_1	4505.84	4496.89	4496.5313	tw
$\nu_2 + \nu_4 + \nu_5$, A_2	4526.31	4506.40		
$\nu_2 + \nu_5 + \nu_7$, B_2	4576.92	4539.76		
$\nu_7 + \nu_8 + \nu_9$, B_1	4556.42	4540.28	4539.7954	tw
$3\nu_7 + \nu_9$, A_2	4515.28	4544.47		
$3\nu_5 + \nu_7$, B_2	5073.56	5070.07		
$2\nu_3 + \nu_8$, B_2	5098.52	5082.69		
$\nu_1 + \nu_4 + \nu_7$, B_1	5089.34	5086.82		
$2\nu_5 + 2\nu_9$, A_1	5083.93	5101.94		
$\nu_1 + 2\nu_7$, A_1	5137.71	5111.12	5111.5773	tw
$\nu_3 + 3\nu_9$, B_2	5117.51	5111.35		
$\nu_4 + \nu_6 + \nu_7$, A_1	5123.44	5121.46		
$\nu_3 + \nu_4 + 2\nu_5$, A_1	5125.25	5125.52		
$2\nu_3 + \nu_4 + \nu_9$, B_2	5123.52	5139.04		
$\nu_6 + 2\nu_7$, B_1	5168.70	5144.12	5142.7189	tw
$4\nu_4 + \nu_7$, B_1	5178.06	5153.08		
$2\nu_3 + \nu_7 + \nu_9$, A_2	5176.65	5161.80		
$\nu_3 + 2\nu_5 + \nu_7$, B_1	5178.61	5162.58		
$\nu_1 + \nu_2$, A_1	5138.89	5170.18	5169.8626	tw
$3\nu_5 + \nu_9$, B_1	5187.96	5199.29		
$\nu_1 + \nu_8$, B_2	5219.11	5204.04	5204.9991	tw
$\nu_2 + \nu_6$, B_1	5175.17	5206.44	5206.9582	tw

TABLE 5 Continued

band	center[83]	center, calc.	center, exp.	ref	band	center[83]	center, calc.	center, exp.	ref
1	2	3	4	5	1	2	3	4	5
$2\nu_4 + 2\nu_5, A_1$	4717.88	4717.51			$\nu_2 + 3\nu_4, A_1$	5244.92	5207.48		
$\nu_2 + \nu_5 + \nu_9, B_1$	4713.27	4721.39			$\nu_3 + \nu_5 + 2\nu_9, A_2$	5211.73	5210.12		
$\nu_3 + \nu_4 + \nu_8, B_2$	4696.04	4734.85	4736.0100	tw	$2\nu_3 + \nu_4 + \nu_5, A_2$	5219.17	5222.97		
$\nu_3 + \nu_7 + \nu_8, A_2$	4758.27	4739.87			$3\nu_4 + \nu_8, B_2$	5274.51	5233.34		
$\nu_3 + 2\nu_4 + \nu_9, B_2$	4723.59	4752.70			$\nu_6 + \nu_8, A_2$	5258.38	5243.03		
$\nu_5 + 2\nu_7 + \nu_9, B_1$	4748.46	4764.05			$2\nu_3 + \nu_5 + \nu_7, B_2$	5266.65	5254.67		
$\nu_5 + \nu_8 + \nu_9, A_2$	4778.65	4768.97			$\nu_1 + \nu_4 + \nu_9, B_2$	5231.17	5255.85	5256.4396	tw
$\nu_7 + 3\nu_9, A_2$	4784.08	4775.23			$\nu_2 + 2\nu_4 + \nu_7, B_1$	5315.08	5260.63		
$\nu_4 + 2\nu_5 + \nu_7, B_1$	4786.93	4783.03			$3\nu_4 + 2\nu_7, A_1$	5262.31	5265.34		
$\nu_2 + 2\nu_5, A_1$	4810.05	4796.09			$3\nu_3 + \nu_4, A_1$	5296.09	5286.90		
$\nu_3 + \nu_4 + \nu_7 + \nu_9, A_2$	4792.42	4797.87			$\nu_4 + \nu_6 + \nu_9, A_2$	5263.08	5291.96		
$\nu_3 + 2\nu_7 + \nu_9, B_2$	4847.04	4803.60			$2\nu_2 + \nu_4, A_1$	5342.64	5292.64		
$\nu_4 + \nu_5 + 2\nu_9, A_2$	4805.72	4817.97			$4\nu_5, A_1$	5296.38	5294.19		
$\nu_3 + 2\nu_4 + \nu_5, A_2$	4822.76	4839.42			$\nu_1 + \nu_7 + \nu_9, A_2$	5289.53	5296.72		
$\nu_2 + \nu_3 + \nu_9, B_2$	4832.94	4854.31	4854.4146	tw	$\nu_3 + 2\nu_5 + \nu_9, B_2$	5310.33	5316.05		
$2\nu_5 + 2\nu_7, A_1$	4841.80	4855.34			$\nu_6 + \nu_7 + \nu_9, B_2$	5318.32	5317.89	5318.5860	tw
$\nu_5 + \nu_7 + 2\nu_9, B_2$	4876.19	4867.60			$2\nu_3 + 2\nu_9, A_1$	5322.53	5320.08		
$4\nu_9, A_1$	4889.01	4874.38			$\nu_1 + \nu_4 + \nu_5, A_2$	5323.39	5326.82		
$2\nu_5 + \nu_8, B_2$	4884.37	4881.50			$2\nu_4 + \nu_7 + \nu_8, A_2$	5362.15	5327.76		
$\nu_3 + \nu_4 + \nu_5 + \nu_7, B_2$	4885.95	4887.49			$3\nu_3 + \nu_7, B_1$	5337.72	5328.21		
$\nu_3 + \nu_4 + 2\nu_9, A_1$	4927.48	4889.93			$4\nu_4 + \nu_9, B_2$	5309.32	5332.51		
$\nu_2 + \nu_3 + \nu_5, A_2$	4924.28	4895.98			$2\nu_4 + 3\nu_7, B_1$	5332.35	5353.10		
$2\nu_3 + 2\nu_4, A_1$	4910.65	4902.61			$2\nu_2 + \nu_7, B_1$	5384.50	5356.85		
$\nu_4 + 2\nu_5 + \nu_9, B_2$	4907.84	4928.61			$\nu_2 + \nu_4 + \nu_8, B_2$	5373.68	5356.95		
$\nu_3 + \nu_5 + 2\nu_7, A_2$	4934.95	4949.22			$\nu_2 + \nu_4 + 2\nu_7, A_1$	5371.04	5361.90		
$2\nu_3 + \nu_4 + \nu_7, B_1$	4967.98	4952.29			$\nu_4 + \nu_5 + \nu_6, B_2$	5358.87	5364.11		
$\nu_3 + \nu_8 + \nu_9, A_1$	4899.65	4954.82	4955.2927	tw	$\nu_1 + \nu_5 + \nu_7, B_2$	5376.13	5378.54		
$\nu_5 + 3\nu_9, B_1$	4984.29	4968.02			$4\nu_4 + \nu_5, A_2$	5414.44	5403.59		
$2\nu_3 + 2\nu_7, A_1$	5011.11	4977.93			$3\nu_4 + \nu_7 + \nu_9, A_2$	5403.56	5411.08		
$2\nu_5 + \nu_7 + \nu_9, A_2$	4972.68	4979.73			$\nu_5 + \nu_6 + \nu_7, A_2$	5408.48	5411.25		
$\nu_3 + \nu_7 + 2\nu_9, B_1$	4992.10	4989.70			$\nu_3 + 3\nu_5, A_2$	5413.31	5412.09		
$\nu_3 + \nu_5 + \nu_8, B_1$	4999.94	5002.36			$\nu_2 + \nu_7 + \nu_8, A_2$	5433.03	5415.78		
$\nu_4 + 3\nu_5, A_2$	5014.34	5015.18			$2\nu_3 + \nu_5 + \nu_9, B_1$	5415.70	5415.79		
$\nu_2 + 2\nu_3, A_1$	5021.53	5024.54			$\nu_4 + 2\nu_8, A_1$	5458.77	5420.82		
$\nu_1 + 2\nu_4, A_1$	5026.76	5039.59	5039.5485	tw	$\nu_4 + 2\nu_7 + \nu_8, B_2$	5435.59	5422.23		
$\nu_3 + \nu_4 + \nu_5 + \nu_9, B_1$	5024.18	5042.37			$\nu_1 + 2\nu_9, A_1$	5421.71	5427.04		
$5\nu_4, A_1$	5079.62	5056.75			$\nu_1 + \nu_3 + \nu_4, A_1$	5430.85	5439.97		
$2\nu_4 + \nu_6, B_1$	5064.00	5063.69			$\nu_4 + 4\nu_7, A_1$	5388.21	5445.38		
$\nu_3 + \nu_5 + \nu_7 + \nu_9, A_1$	5083.16	5064.36			$\nu_2 + 2\nu_4 + \nu_9, B_2$	5455.30	5446.49		
$\nu_6 + 2\nu_9, B_1$	5448.30	5446.68	5446.5963	tw	$\nu_3 + \nu_4 + 3\nu_7, B_1$	5716.88	5733.46		
$\nu_3 + \nu_4 + \nu_6, B_1$	5452.55	5457.54			$\nu_5 + 2\nu_8, A_2$	5767.53	5738.03		
$\nu_1 + \nu_3 + \nu_7, B_1$	5477.73	5474.39			$\nu_5 + 2\nu_7 + \nu_8, B_1$	5737.70	5742.02		
$3\nu_7 + \nu_8, A_2$	5494.83	5484.89			$\nu_5 + 4\nu_7, A_2$	5683.68	5742.71		
$2\nu_4 + \nu_8 + \nu_9, A_1$	5490.07	5486.96			$\nu_3 + \nu_5 + \nu_6, B_2$	5739.02	5744.49		
$\nu_2 + 3\nu_7, B_1$	5412.80	5488.06			$\nu_7 + \nu_8 + 2\nu_9, A_2$	5770.99	5750.23		
$3\nu_4 + \nu_5 + \nu_7, B_2$	5503.04	5489.29			$\nu_2 + \nu_3 + 2\nu_7, A_1$	5753.45	5750.60		
$\nu_3 + \nu_6 + \nu_7, A_1$	5496.30	5495.31			$\nu_2 + \nu_4 + \nu_5 + \nu_9, B_1$	5746.61	5752.88		
$2\nu_4 + 2\nu_7 + \nu_9, B_2$	5483.59	5498.57			$2\nu_4 + 3\nu_9, B_2$	5727.13	5754.81		
$3\nu_3 + \nu_9, B_2$	5504.08	5499.08			$\nu_3 + \nu_4 + \nu_7 + \nu_8, A_2$	5775.73	5762.15		
$\nu_3 + 4\nu_4, A_1$	5511.24	5499.32			$\nu_3 + 3\nu_4 + \nu_9, B_2$	5736.08	5771.72		
$2\nu_2 + \nu_9, B_2$	5533.67	5504.58			$\nu_3 + 4\nu_7, A_1$	5757.03	5772.22		
$2\nu_3 + 2\nu_5, A_1$	5513.25	5510.44			$3\nu_7 + 2\nu_9, B_1$	5752.66	5773.40		
$\nu_2 + \nu_4 + \nu_7 + \nu_9, A_2$	5521.24	5512.01			$\nu_2 + \nu_3 + \nu_8, B_2$	5785.16	5790.66		
$\nu_7 + 2\nu_8, B_1$	5535.60	5519.00			$\nu_4 + \nu_5 + \nu_8 + \nu_9, A_2$	5795.52	5800.32		
$\nu_1 + \nu_5 + \nu_9, B_1$	5511.46	5524.52			$\nu_4 + \nu_5 + 2\nu_7 + \nu_9, B_1$	5782.40	5803.48		
$\nu_2 + 2\nu_4 + \nu_5, A_2$	5552.58	5528.52			$\nu_1 + 2\nu_3, A_1$	5815.57	5806.56	5806.5300	tw
$\nu_5 + \nu_6 + \nu_9, A_1$	5541.61	5548.09	5547.7442	tw	$2\nu_4 + 2\nu_5 + \nu_7, B_1$	5813.60	5806.90		
$\nu_2 + 2\nu_7 + \nu_9, B_2$	5572.99	5560.85			$\nu_3 + 2\nu_7 + \nu_8, B_2$	5833.48	5813.70		
$\nu_2 + \nu_8 + \nu_9, A_1$	5569.91	5562.51	5562.1906	tw	$\nu_4 + \nu_7 + 3\nu_9, A_2$	5812.96	5818.82		
$\nu_4 + \nu_7 + \nu_8 + \nu_9, B_1$	5573.50	5563.18			$2\nu_3 + \nu_6, B_1$	5821.74	5819.28	5819.1679	tw
$\nu_3 + 3\nu_4 + \nu_7, B_1$	5593.98	5570.18			$\nu_2 + \nu_5 + \nu_7 + \nu_9, A_1$	5802.72	5825.01		
$3\nu_4 + 2\nu_9, A_1$	5525.16	5578.68			$\nu_2 + 3\nu_9, B_2$	5834.44	5826.58		
$2\nu_4 + \nu_5 + \nu_8, B_1$	5596.30	5579.93			$\nu_3 + 2\nu_4 + \nu_7 + \nu_9, A_2$	5814.60	5829.99		
$\nu_4 + 3\nu_7 + \nu_9, A_2$	5549.44	5581.60			$\nu_2 + \nu_4 + 2\nu_5, A_1$	5845.81	5830.18		
$2\nu_4 + \nu_5 + 2\nu_7, A_2$	5577.45	5586.23			$2\nu_4 + \nu_5 + 2\nu_9, A_2$	5827.44	5840.97		
$2\nu_2 + \nu_5, A_2$	5623.13	5589.16			$\nu_2 + \nu_3 + \nu_4 + \nu_9, B_2$	5864.23	5846.30		
$3\nu_3 + \nu_5, A_2$	5596.20	5592.03			$\nu_8 + 3\nu_9, A_1$	5879.60	5849.73		
$\nu_1 + 2\nu_5, A_1$	5605.60	5610.55			$\nu_3 + 3\nu_4 + \nu_5, A_2$	5837.66	5860.02		
$\nu_3 + 2\nu_4 + 2\nu_7, A_1$	5662.53	5615.01			$\nu_5 + \nu_7 + \nu_8 + \nu_9, B_2$	5869.12	5860.90		
$2\nu_8 + \nu_9, B_2$	5660.20	5630.89	5631.3137	tw	$\nu_2 + 2\nu_5 + \nu_7, B_1$	5896.29	5863.01		

TABLE 5 Continued

band	center[83]	center, calc.	center, exp.	ref	band	center[83]	center, calc.	center, exp.	ref
1	2	3	4	5	1	2	3	4	5
$2\nu_7 + \nu_8 + \nu_9, A_1$	5642.74	5634.98			$2\nu_1, A_1$	5889.44	5867.94	5867.8242	tw
$\nu_1 + \nu_3 + \nu_9, B_2$	5630.38	5637.91			$\nu_5 + 3\nu_7 + \nu_9, A_1$	5838.41	5870.08		
$2\nu_5 + \nu_6, B_1$	5639.32	5645.89			$\nu_3 + 2\nu_8, A_1$	5885.72	5870.25		
$2\nu_4 + \nu_7 + 2\nu_9, B_1$	5615.19	5646.40			$\nu_2 + \nu_3 + \nu_7 + \nu_9, A_2$	5914.48	5875.52		
$\nu_3 + \nu_6 + \nu_9, A_2$	5646.75	5649.32			$\nu_1 + \nu_6, B_1$	5865.01	5878.56	5878.4563	tw
$\nu_2 + \nu_4 + 2\nu_9, A_1$	5651.80	5650.13			$\nu_3 + \nu_4 + 2\nu_7 + \nu_9, B_2$	5878.94	5880.61		
$3\nu_4 + \nu_5 + \nu_9, B_1$	5627.80	5651.73			$\nu_4 + 2\nu_5 + \nu_8, B_2$	5903.66	5881.36		
$4\nu_7 + \nu_9, B_2$	5601.09	5653.08			$\nu_4 + 2\nu_5 + 2\nu_7, A_1$	5878.36	5889.17		
$\nu_2 + \nu_5 + 2\nu_7, A_2$	5659.02	5653.26			$2\nu_7 + 3\nu_9, B_2$	5884.59	5898.84		
$\nu_2 + \nu_3 + 2\nu_4, A_1$	5658.74	5653.98			$\nu_3 + 2\nu_4 + \nu_5 + \nu_7, B_2$	5910.56	5902.84		
$\nu_2 + \nu_5 + \nu_8, B_1$	5668.31	5655.35			$\nu_3 + \nu_4 + \nu_8 + \nu_9, A_1$	5914.47	5904.84		
$4\nu_3, A_1$	5662.15	5657.46			$\nu_2 + \nu_5 + 2\nu_9, A_2$	5926.79	5915.42		
$\nu_2 + \nu_3 + \nu_4 + \nu_7, B_1$	5713.20	5665.83			$\nu_3 + 2\nu_4 + 2\nu_9, A_1$	5947.02	5921.16		
$\nu_2 + \nu_4 + \nu_5 + \nu_7, B_2$	5612.90	5666.77			$\nu_3 + 3\nu_7 + \nu_9, A_2$	5929.08	5927.41		
$\nu_4 + \nu_8 + 2\nu_9, B_2$	5691.77	5671.10			$\nu_4 + \nu_5 + \nu_7 + 2\nu_9, B_2$	5907.50	5933.60		
$\nu_4 + \nu_5 + \nu_7 + \nu_8, A_1$	5674.10	5673.72			$\nu_5 + \nu_8 + 2\nu_9, B_1$	5980.88	5945.63		
$\nu_2 + \nu_7 + 2\nu_9, B_1$	5713.54	5677.06			$\nu_2 + \nu_3 + \nu_4 + \nu_5, A_2$	5958.00	5949.38		
$2\nu_4 + \nu_5 + \nu_7 + \nu_9, A_1$	5712.20	5677.51			$2\nu_4 + 2\nu_5 + \nu_9, B_2$	5931.86	5950.86		
$\nu_3 + 2\nu_4 + \nu_8, B_2$	5703.80	5705.83			$\nu_4 + 4\nu_9, A_1$	5915.25	5951.66		
$\nu_4 + 2\nu_7 + 2\nu_9, A_1$	5691.02	5713.89			$2\nu_5 + 3\nu_7, B_1$	5928.54	5958.48		
$\nu_1 + \nu_3 + \nu_5, A_2$	5719.08	5722.00			$\nu_2 + \nu_3 + \nu_5 + \nu_7, B_2$	6002.62	5958.94		
$2\nu_2 + \nu_3, A_1$	5738.65	5727.99			$\nu_3 + \nu_4 + \nu_5 + 2\nu_7, A_2$	5969.27	5961.85		
$3\nu_4 + 2\nu_5, A_1$	5734.82	5731.82			$\nu_3 + \nu_7 + \nu_8 + \nu_9, B_1$	5982.21	5971.18		
$2\nu_3 + 2\nu_4 + \nu_7, B_1$	5990.54	5975.31			$\nu_3 + \nu_4 + \nu_7 + 2\nu_9, B_1$	6021.35	6026.89		
$2\nu_5 + \nu_7 + \nu_8, A_2$	5971.62	5984.00			$2\nu_3 + \nu_4 + 2\nu_7, A_1$	6043.38	6027.74		
$\nu_7 + 4\nu_9, B_1$	5996.86	5986.36			$\nu_2 + 2\nu_3 + \nu_4, A_1$	6053.19	6033.46		
$2\nu_3 + 3\nu_4, A_1$	5923.51	5992.03			$2\nu_4 + 3\nu_5, A_2$	6040.79	6041.35		
$\nu_5 + 2\nu_7 + 2\nu_9, A_2$	5973.49	5992.92			$\nu_2 + 2\nu_5 + \nu_9, B_2$	6023.51	6042.11		
$2\nu_6, A_1$	5952.76	5999.07	5998.9646	tw	$\nu_2 + \nu_3 + 2\nu_9, A_1$	6055.86	6052.32		
$\nu_4 + \nu_5 + 3\nu_9, B_1$	6012.95	6001.15			$\nu_3 + 2\nu_4 + \nu_5 + \nu_9, B_1$	6046.15	6055.02		
$\nu_1 + 3\nu_4, A_1$	6040.63	6002.61			$\nu_3 + \nu_5 + \nu_7 + \nu_8, A_1$	6079.28	6064.52		
$\nu_3 + \nu_5 + 3\nu_7, B_2$	6013.78	6015.46			$2\nu_3 + 3\nu_7, B_1$	6082.03	6073.52		
$\nu_4 + 2\nu_5 + \nu_7 + \nu_9, A_2$	6006.48	6021.66			$\nu_1 + \nu_4 + \nu_8, B_2$	6235.33	6209.51	6208.2925	tw
$\nu_3 + \nu_4 + \nu_5 + \nu_8, B_1$	6017.18	6026.54			$\nu_2 + \nu_6 + \nu_7, A_1$	6249.37	6298.83	6298.9003	tw

[a] Values presented in column 2 were calculated with the parameters from Tables I (cc-pVQZ) and VI of ref 83. Band centers presented in column 3 were calculated with the parameters from Tables 6 and 7 of the present paper. Experimental values of the band centers are given in column 4. tw (this work) indicates results obtained in the present investigation. [b] Was not used in the fit (see discussion in the text).

TABLE 6: F_{ij} Parameters of the Methane Molecule

parameter	present work	ref 83	ref 35
F_{11}/aJ Å^{-2}	5.47384[a]	5.47384	5.43512
F_{22}/aJ	0.578602(332)[b])	0.57770	0.58401
F_{33}/aJ Å^{-2}	5.387874(832)	5.37696	5.37813
F_{34}/aJ Å^{-1}	−0.21057[a]	−0.21057	−0.22100
F_{44}/aJ	0.533740(416)	0.53225	0.54801
number of experimental band centers		89	
number of fitted parameters		47	
d_{rms}		0.67 cm^{-1}	

[a] Constrained to the value from ref 83. [b] For uncertainties, see caption to Table 4 and discussion in Section 5.

outdated. The problems of ab initio theory in predicting poorly the experimental band centers therefore reside largely in the anharmonic part of the potential. At this point, one might be tempted to point to the in part large discrepancies between experiment and ab initio theory for the anharmonic constants in Table 7. However, the two sets of constants have a somewhat different physical significance. Whereas the constants of our model are effective Hamiltonian constants obtained from a direct fit to experimental band centers, the anharmonic constants of Lee, Martin, and Taylor are derived from the anharmonic ab initio potential by means of low-order perturbation theory. To compare our anharmonic constants with the ab initio potential of Lee, Martin, and Taylor at the appropriate level of significance, one would have to carry out 9-dimensional vibrational variational calculations on the potential of Lee, Martin, and Taylor and then fit the corresponding calculated band centers (or level positions) with the same effective Hamiltonian as used for the fit to experiment (see also the corresponding discussion in ref 31). The large discrepancies between experimental and theoretical level positions have thus two conceptually quite different origins: They arise

(i) from the errors in the ab initio potential hypersurface and

(ii) from errors in using expressions based on low-order perturbation theory in calculating level positions from anharmonic potential coefficients.

Without carrying out the theoretical program discussed above, it is not easy to separate the different ab initio errors and identify their relative magnitude. Anharmonic constants from the potential of refs 37 and 38 have not been published in detail, thus a direct comparison is not easy. We note, however, that the variational calculations of refs 40−42 on that potential for $\nu_2 + 2\nu_3$ of CH_4 differ by more than 10 cm^{-1} from the precise experimental result for this level ($J = 0$, F_2 or F_1^- in S_4^* at 7510.3378 ± 0.001 cm^{-1}).[65] This thus provides an estimate of the intrinsic errors in that potential.

We might mention here also some simple theoretical models which have been proposed to describe the anharmonic level structure of CH_2D_2 in relation to some gas phase[86] and liquid Argon solution experiments.[87] Neither of these is very successful in giving an accurate description. Independent from the theoretical analysis, however, the experimental spectra of CH_2D_2 in liquid Argon solution between 94 and 101 K[87] provide an interesting comparison with our low-temperature gas phase spectra in terms of the shifts

TABLE 7: Vibrational Spectroscopic Parameters of the CH_2D_2 Molecule (in cm^{-1})

parameter	this work	ref 83	parameter	this work	ref 83
1	2	3	1	2	3
ω_1	3104.4217[a]	3102.5	x_{38}	−3.903(387)	−3.067
ω_2	2237.9855[a]	2236.9	x_{39}	−0.1829(240)	0.651
ω_3	1472.3115[a]	1470.9	x_{44}	−5.207(148)	−4.492
ω_4	1054.4405[a]	1053.1	x_{45}	1.4696(165)	0.512
ω_5	1361.2375[a]	1360.1	x_{46}	−1.1383(410)	−1.411
ω_6	3159.7912[a]	3156.5	x_{47}	−0.868(479)	0.727
ω_7	1117.7847[a]	1116.2	x_{48}	−15.620[b]	−15.620
ω_8	2339.5713[a]	2337.1	x_{49}	−2.5710(516)	−1.914
ω_9	1267.4576[a]	1265.7	x_{55}	−2.648(122)	−2.211
x_{11}	−25.3041(812)[c]	−27.344	x_{56}	−11.912(248)	−12.869
x_{12}	−3.294(858)	−0.831	x_{57}	0.385[b]	0.385
x_{13}	−15.2348(957)	−7.251	x_{58}	−9.655[b]	−9.655
x_{14}	−2.4222(828)	−2.052	x_{59}	−9.6710(420)	−8.755
x_{15}	−11.752[b]	−11.752	x_{66}	−31.566(151)	−31.640
x_{16}	−114.112(378)	−115.079	x_{67}	−11.062(496)	−11.273
x_{17}	−7.765(441)	−8.786	x_{68}	3.715[b]	3.715
x_{18}	−9.216(452)	0.403	x_{69}	−12.732(178)	−10.822
x_{19}	−0.621(578)	−6.139	x_{77}	−6.587(602)	−1.879
x_{22}	−10.451(540)	−14.130	x_{78}	−7.001[b]	−7.001
x_{23}	−3.609(264)	−2.065	x_{79}	2.464(468)	3.590
x_{24}	−0.568(439)	0.849	x_{88}	−15.2572(438)	−18.583
x_{25}	−7.320[b]	−7.320	x_{89}	−9.145(858)	−15.620
x_{26}	−0.509[b]	−0.509	x_{99}	−5.2575(453)	−4.354
x_{27}	−1.75(158)	−8.016	y_{777}	0.6657(525)	-
x_{28}	−58.0734(996)	−59.737	k_{277}	61.406(207)	-
x_{29}	−7.677(392)	−4.344	δ_{277}	−1.275(948)	-
x_{33}	−5.1914(976)	−6.733	k_{489}	68.717(321)	-
x_{34}	−1.9829(885)	−1.539	γ_{3499}	13.888(169)	-
x_{35}	−0.447[b]	−0.447	k_{133}	−42.61(108)	-
x_{36}	−21.507(175)	−22.147	γ_{3759}	40.44(104)	-
x_{37}	−7.307(164)	−7.529	γ_{1166}	124.562(591)	-

[a] Was not fitted but calculated on the basis of the F_{ij} parameters given in column 2 of Table 6. [b] Constrained to the value from ref 83. [c] Uncertainties are stated in parentheses in terms of one standard deviation of the last digit given (see Section 5).

of the bands in solution in a liquid weakly interacting "rare-gas" solvent compared to the gas phase, the shifts being quite appreciable.

6. Conclusions and Outlook

We have demonstrated here that by means of spectra taken with high, Doppler limited resolution at low temperatures around 80 K one can accurately locate a large number of vibrational levels for CH_2D_2, using the technique of specific assignment of $J' = 0 \leftarrow J'' = 1$ transitions, which provides pure vibrational level energies. 71 vibrational energies including excitations up to and exceeding 6000 (hc) cm^{-1} were thus combined with previously known vibrational band centers to provide a large data set of 93 vibrational energies. An effective Hamiltonian with 47 parameters adjusted to fit these data describes this spectrum with a root-mean-square deviation of less than 0.7 cm^{-1} and no deviations exceeding 2 cm^{-1}. A complete list of about 350 levels below 6300 cm^{-1} can thus be accurately calculated and should have good reliability over this whole energy range, extendable by extrapolation to higher energies, at least for heuristic purposes. Indeed, the predicted level positions should be helpful in assigning further vibrational levels in future work. Furthermore one can derive an empirical potential function for methane using these data.[76]

The corresponding level energies in Table 5 can be used as a benchmark for ab initio calculations. For instance, we find that level energies calculated from parameters based on the ab initio calculations of Lee, Martin, and Taylor[83] frequently differ from the experimental results by more than 20 cm^{-1}, where the discrepancy arises in part from the ab initio potential and in part from the use of low-order perturbation theoretical expressions in the calculations of ref 83.

In future work, it should also be possible to compare with 9-dimensional vibrational variational calculations similar to those reported for CH_4 in refs 40−43 using appropriate full dimensional potential hypersurfaces.[35−38] Adjustment of parameters of such global analytical potentials[35,36] should enable us then to refine the available potentials. These refined potential hypersurfaces can subsequently be used for quantum-dynamical wavepacket calculations, for instance, with coherent infrared multiphoton excitation for various methane isotopomers[34,45] or for accurate calculations of statistical thermodynamical and kinetics properties based on vibrational densities of states in the methane system. Of course, some of these applications can also be directly based on the experimental and empirical effective Hamiltonian results shown in Table 5.

While level positions in Table 5 are accurate, it should be understood that the assignment of normal mode excitations ($\nu_i + \nu_j + \nu_k$) has only an approximate meaning of very limited significance, when there is strong mixing, which we have in fact identified by some of the coupling parameters in Table 6. However, assigned level symmetries are robust and can for instance be used for testing the convergence to symmetry distributions in level densities following.[88] Finally, the present results provide a starting point for a global rovibrational analysis including rovibrational levels to higher J-values with extensive anharmonic and Coriolis couplings.[76] Through a combination with similar results for other isotopomers $^{12}CH_4$,[63] $^{13}CH_4$,[64] CH_3D, and CD_3H,[31,89,90] one can obtain a consistent global description of spectra and dynamics of the stable isotopomers of methane.

Acknowledgment. We enjoyed discussion with Fabio Mariotti, Hans Martin Niederer, and Roberto Marquardt. Our work is supported financially by the ETH Zürich and the Schweizerischer Nationalfonds. O.N.U. and E.S.B. are also supported by a PICS grant. We enjoyed many years of friendly scientific exchange with Max Wolfsberg.

Appendix

TABLE A1: Lowest Ground-State Combination Differences of the CH_2D_2 Molecule (in cm^{-1})[a]

	value/cm^{-1}		d_{rms}[a]			value/cm^{-1}		d_{rms}[a]	
$J'K_a'K_c' - J''K_a''K_c''$	fit.	exp.[a]	10^4 cm^{-1}	n[b]	$J'K_a'K_c' - J''K_a''K_c''$	fit.	exp.[a]	10^4 cm^{-1}	n[b]
1	2	3	4	5	1	2	3	4	5
2 2 0 − 2 0 2	4.39224	4.39222	1.7	68	5 2 4 − 4 2 2	30.79386	30.79389	1.0	62
3 2 1 − 3 0 3	5.40865	5.40869	1.8	81	4 2 3 − 3 0 3	30.84926	30.84928	1.1	83
4 3 1 − 4 1 3	6.93612	6.93615	1.8	58	6 1 6 − 5 1 4	31.21071	31.21072	1.4	23
3 3 0 − 3 1 2	7.05255	7.05259	2.1	67	3 1 3 − 1 1 1	31.55448	31.55441	1.2	51
4 2 2 − 4 0 4	7.26937	7.26934	1.9	53	3 0 3 − 1 0 1	32.11883	32.11880	0.8	42
5 3 2 − 5 1 4	7.48927	7.48924	1.2	29	6 1 5 − 5 3 3	32.25480	32.25466	1.3	15
6 3 3 − 6 1 5	8.99002	8.99009	1.4	9	5 3 3 − 4 3 1	32.81639	32.81635	1.2	60
6 4 2 − 6 2 4	9.58088	9.58089	1.1	10	5 4 2 − 4 4 0	33.07648	33.07667	1.8	31
3 3 1 − 3 1 3	9.72255	9.72255	2.2	43	5 4 1 − 4 5 1	33.12952	33.12941	1.8	45
5 2 3 − 5 0 5	9.87175	9.87174	1.9	29	4 3 2 − 3 1 2	33.45682	33.45687	1.1	77
5 4 1 − 5 2 3	10.13182	10.13190	1.8	32	5 3 2 − 4 3 2	33.73420	33.73414	1.4	62
4 4 0 − 4 2 2	10.88372	10.88369	2.3	33	3 1 2 − 1 1 0	33.80009	33.80007	0.8	36
4 3 2 − 4 1 4	11.07795	11.07799	2.4	62	5 2 3 − 4 2 3	35.51663	35.51666	1.1	57
2 1 2 − 1 1 0	12.19917	12.19921	1.0	71	6 2 5 − 5 2 3	35.59931	35.59930	1.2	22
4 4 1 − 4 2 3	12.51893	12.51889	1.7	43	4 3 1 − 3 1 3	36.36331	36.36325	1.2	37
5 3 3 − 5 1 5	12.88537	12.88538	0.7	24	5 1 4 − 4 1 4	37.32288	37.32280	1.3	73
5 4 2 − 5 2 4	13.16633	13.16636	1.7	27	3 2 1 − 1 0 1	37.52748	37.52754	1.0	28
2 1 1 − 1 1 1	14.02211	14.02210	1.7	82	4 4 1 − 3 2 1	37.95954	37.95955	1.4	39
6 4 3 − 6 2 5	14.22886	14.22875	2.8	10	5 2 4 − 4 0 4	38.06323	38.06317	1.2	53
6 5 1 − 6 3 3	14.38942	14.38948	1.0	8	4 4 0 − 3 2 2	38.61987	38.61986	1.5	36
3 0 3 − 2 2 1	14.90957	14.90955	1.5	63	6 3 4 − 5 3 2	38.81953	38.81948	0.9	24
3 3 0 − 4 1 4	15.32632	15.32633	2.6	32	6 4 3 − 5 4 1	39.69636	39.69640	0.7	15
5 5 1 − 5 3 3	15.94298	15.94294	0.6	12	5 3 3 − 4 1 3	39.75251	39.75246	1.3	48
2 2 1 − 1 0 1	17.20926	17.20924	1.6	68	6 4 2 − 5 4 2	39.96171	39.96171	2.1	17
3 1 3 − 2 1 1	17.53237	17.53238	1.4	88	4 0 4 − 2 2 0	39.98343	39.98339	1.6	13
3 2 2 − 2 2 0	19.51965	19.51661	1.2	80	3 3 0 − 1 1 0	40.85264	40.85270	0.8	31
2 0 2 − 0 0 0	19.51965	19.51974	1.3	39	6 3 3 − 5 3 3	41.24482	41.24490	1.3	22
4 1 3 − 3 3 1	19.70464	19.70461	2.0	38	3 3 1 − 1 1 1	41.27704	41.27710	0.7	30
5 2 4 − 4 4 0	19.91015	19.91010	1.8	12	4 4 1 − 3 0 3	43.36819	43.36816	2.2	17
5 1 5 − 4 3 1	19.93102	19.93101	1.7	18	6 2 4 − 5 2 4	43.54716	43.54716	1.4	26
5 4 1 − 5 0 5	20.00356	20.00359	1.5	9	5 4 2 − 4 2 2	43.96019	43.96022	1.8	39
3 2 1 − 2 2 1	20.31822	20.31823	1.4	78	4 1 4 − 2 1 2	43.97978	43.97978	0.4	38
4 0 4 − 3 2 2	20.46679	20.46676	1.8	56	4 0 4 − 2 0 2	44.37568	44.37566	0.5	33
3 1 2 − 2 1 2	21.60091	21.60090	1.6	98	5 3 2 − 4 1 4	44.81215	44.81214	1.0	40
4 1 4 − 3 1 2	22.37887	22.37890	1.7	79	6 1 5 − 5 1 5	45.14017	45.14023	1.2	20
5 2 3 − 4 4 1	22.99770	22.99783	1.7	20	6 2 5 − 5 0 5	45.47106	45.47117	1.6	21
3 2 2 − 2 0 2	23.90889	23.90890	1.3	67	5 4 1 − 4 2 3	45.64845	45.64846	1.1	40
2 2 0 − 0 0 0	23.91189	23.91190	0.9	31	4 2 3 − 2 2 1	45.75883	45.75879	0.8	35
4 2 3 − 3 2 1	25.44061	25.44060	1.7	99	6 3 4 − 5 1 4	46.30880	46.30870	1.7	23
5 0 5 − 4 2 3	25.64489	25.64487	1.1	44	4 1 3 − 2 1 1	46.95957	46.95957	1.0	38
4 3 2 − 3 3 0	26.40427	26.40426	1.6	74	4 2 2 − 2 2 0	47.25280	47.25283	0.6	29
4 3 1 − 3 3 1	26.64076	26.64078	1.9	69	5 5 1 − 4 3 1	48.75938	48.75924	1.3	21
5 1 5 − 4 1 3	26.86714	26.86713	1.4	50	5 5 0 − 4 3 2	48.96530	48.96522	1.5	26
3 3 1 − 2 1 1	27.25493	27.25497	0.9	43	6 4 3 − 5 2 3	49.82817	49.82820	1.4	17
4 2 2 − 3 2 2	27.73615	27.73613	1.2	92	5 0 5 − 3 2 1	51.08549	51.08552	1.2	17
3 3 0 − 2 1 2	28.65346	28.65354	0.8	57	5 4 2 − 4 0 4	51.22956	51.22941	1.7	15
4 1 3 − 3 1 3	29.42719	29.42710	1.4	98	4 2 2 − 2 0 2	51.64504	51.64509	1.7	29
5 1 4 − 3 3 0	52.64919	52.64938	1.6	14	5 3 3 − 3 1 3	69.17960	69.17960	1.3	30
6 4 2 − 5 2 4	53.12804	53.12801	1.3	15	5 4 1 − 3 2 1	71.08905	71.08900	1.2	28
4 3 1 − 2 1 1	53.89569	53.89558	1.8	31	6 2 5 − 4 2 3	71.11595	71.11601	0.9	28
6 5 2 − 5 3 2	54.91218	54.91233	0.9	14	5 4 2 − 3 2 2	71.69634	71.69629	1.3	27
4 3 2 − 2 1 2	55.05773	55.05776	1.6	26	6 1 5 − 4 1 3	72.00731	72.00740	1.1	25
6 5 1 − 5 3 3	55.63424	55.63413	1.5	11	6 3 4 − 4 3 2	72.55373	72.55369	1.7	22
5 1 5 − 3 1 3	56.29433	56.29427	1.4	38	6 4 3 − 4 4 1	72.82588	72.82579	0.9	11
5 0 5 − 3 0 3	56.49414	56.49406	1.4	39	6 4 2 − 4 4 0	73.03818	73.03812	1.4	9
4 4 0 − 2 2 0	58.13652	58.13653	0.9	25	6 3 3 − 4 3 1	74.06121	74.06125	1.6	20
4 4 1 − 2 2 1	58.27776	58.27784	0.8	25	6 2 4 − 4 224	74.34102	74.34102	1.8	23
5 2 4 − 3 2 2	58.53002	58.52995	1.4	43	5 5 0 − 3 3 0	75.36957	75.36951	1.7	18
5 3 3 − 3 3 1	59.45715	59.45717	1.8	25	5 5 1 − 3 3 1	75.40014	75.40025	0.9	14
5 1 4 − 3 1 2	59.70175	59.70170	1.8	44	5 4 1 − 3 0 3	76.49771	76.49782	1.6	12
5 3 2 − 3 3 0	60.13847	60.13839	1.7	26	6 3 3 − 4 1 3	80.99733	80.99737	1.5	22
5 2 3 − 3 2 1	60.95724	60.95735	1.3	38	6 2 4 − 4 0 4	81.61039	81.61035	1.9	19
6 1 5 − 4 3 1	65.07119	65.07117	2.2	10	6 3 4 − 4 1 4	83.63168	83.63165	2.2	24
5 2 3 − 3 0 3	66.36589	66.36596	1.5	33	6 4 2 − 4 2 2	83.92190	83.92191	1.5	19
5 3 2 − 3 1 2	67.19102	67.19098	0.8	31	6 4 3 − 4 2 3	85.34481	85.34474	2.0	20
6 1 6 − 4 1 4	68.53358	68.53357	1.1	32	6 5 1 − 4 3 1	88.45063	88.45057	0.8	14
6 0 6 − 4 0 4	68.61493	68.61501	0.8	21	6 5 2 − 4 3 2	88.64638	88.64661	2.2	14

[a] Mean experimental value of the individual GSCD and its rms deviation. [b] Here n is the number of separate experimental GSCD obtained from the analysis of 74 absorption bands of the CH_2D_2 molecule recorded in the present study and used in the determination of the mean term value, and its d_{rms}.

References and Notes

(1) Herzberg, G. *Molecular Spectra and Molecular Structure, Infrared and Raman Spectra of Polyatomic Molecules*, 1st ed.; van Nostrand: New York, 1945; *Vol. II*.

(2) Herzberg, G. *Molecular Spectra and Molecular Structure: Electronic Spectra and Electronic Structure of Polyatomic Molecules*; van Nostrand: Toronto, 1966; *Vol. III*.

(3) Wilson, E. B.; Decius, J. C.; Cross, P. C. *Molecular vibrations. The theory of infrared and Raman vibrational spectra*; McGraw-Hill: New York, 1955.

(4) Nielsen, H. H. *Phys. Rev.* **1941**, *60*, 794–810.

(5) Nielsen, H. H. *Phys. Rev.* **1945**, *68*, 181–191.

(6) Nielsen, H. H. *Rev. Mod. Phys.* **1951**, *23*, 90–136.

(7) Amat, G.; Nielsen, H. H.; Tarrago, G. *Rotation-vibration of polyatomic molecules: higher order energies and frequencies of spectral transitions*; Dekker: New York, 1971.

(8) Amat, G.; Goldsmith, M. *J. Chem. Phys.* **1955**, *23*, 1171–1172.

(9) Amat, G. *Cahiers Phys.* **1957**, *11*, 25.

(10) Mills, I. M. *A specialist periodical report/Royal Society of Chemistry. Theoretical chemistry.* **1974**; Vol. 1, p 110.

(11) Papousek, D.; Aliev, M. R. *Stud. Phys. Theor. Chem.* **1982**, *17*, 160.

(12) Califano, S. *Vibrational states*; Wiley: London etc., 1976.

(13) Chen, C. L.; Maessen, B.; Wolfsberg, M. *J. Chem. Phys.* **1985**, *83*, 1795–1807.

(14) Maessen, B.; Wolfsberg, M.; Harding, L. B. *J. Phys. Chem.* **1985**, *89*, 3324–3325.

(15) Maessen, B.; Wolfsberg, M. *J. Phys. Chem.* **1985**, *89*, 3876–3879.

(16) Maessen, B.; Wolfsberg, M. *J. Chem. Phys.* **1984**, *80*, 4651–4662.

(17) Partridge, H.; Schwenke, D. W. *J. Chem. Phys.* **1997**, *106*, 4618–4639.

(18) Schwenke, D. W.; Partridge, H. *J. Chem. Phys.* **2000**, *113*, 6592–6597.

(19) Shirin, S. V.; Polyansky, O. L.; Zobov, N. F.; Ovsyannikov, R. I.; Csaszar, A. G.; Tennyson, J. *J. Mol. Spectrosc.* **2006**, *236*, 216–223.

(20) Maksyutenko, P.; Rizzo, T. R.; Boyarkin, O. V. *J. Chem. Phys.* **2006**, *125*, 181101.

(21) Tennyson, J.; Kostin, M. A.; Barletta, P.; Harris, G. J.; Polyansky, O. L.; Ramanlal, J.; Zobov, N. F. *Comput. Phys. Commun.* **2004**, *163*, 85–116.

(22) Luckhaus, D. *J. Chem. Phys.* **2000**, *113*, 1329–1347.

(23) Quack, M.; Suhm, M. A. *J. Chem. Phys.* **1991**, *95*, 28–59.

(24) Klopper, W.; Quack, M.; Suhm, M. A. *Chem. Phys. Lett.* **1996**, *261*, 35–44.

(25) Klopper, W.; Quack, M.; Suhm, M. A. *J. Chem. Phys.* **1998**, *108*, 10096–10115.

(26) Zhang, D. H.; Wu, Q.; Zhang, J. Z. H.; von Dirke, M.; Bacic, Z. *J. Chem. Phys.* **1995**, *102*, 2315–2325.

(27) Kuhn, B.; Rizzo, T. R.; Luckhaus, D.; Quack, M.; Suhm, M. A *J. Chem. Phys.* **1999**, *111*, 2565–2587; 135 pages of supplementary material published as AIP Document No PAPS JCPS A6-111-302905 by American Institute of Physics, Physics Auxiliary Publication Service, 500 Sunnyside Blvd., Woodbury, N. Y. 1179-29999.

(28) Fehrensen, B.; Luckhaus, D.; Quack, M. *Chem. Phys. Lett.* **1999**, *300*, 312–320.

(29) Fehrensen, B.; Luckhaus, D.; Quack, M. *Chem. Phys.* **2007**, *338*, 90–105.

(30) Peyerimhoff, S. D.; Lewerenz, M.; Quack, M. *Chem. Phys. Lett.* **1984**, *109*, 563–569.

(31) Lewerenz, M.; Quack, M. *J. Chem. Phys.* **1988**, *88*, 5408–5432.

(32) Carrington, T.; Halonen, L.; Quack, M. *Chem. Phys. Lett.* **1987**, *140*, 512–519.

(33) Halonen, L.; Carrington, T.; Quack, M. *J. Chem. Soc., Faraday Trans. 2* **1988**, *84*, 1371–1388.

(34) Marquardt, R.; Quack, M. *J. Chem. Phys.* **1991**, *95*, 4854–4876.

(35) Marquardt, R.; Quack, M. *J. Chem. Phys.* **1998**, *109*, 10628–10643.

(36) Marquardt, R.; Quack, M. *J. Phys. Chem. A* **2004**, *108*, 3166–3181.

(37) Schwenke, D. W.; Partridge, H. *Spectrochim. Acta, Part A* **2001**, *57*, 887–895.

(38) Schwenke, D. W. *Spectrochim. Acta, Part A* **2002**, *58*, 849–861.

(39) Hollenstein, H.; Marquardt, R. R.; Quack, M.; Suhm, M. A. *J. Chem. Phys.* **1994**, *101*, 3588–3602.

(40) Wang, X. G.; Carrington, T. *J. Chem. Phys.* **2003**, *118*, 6260–6263.

(41) Wang, X. G.; Carrington, T. *J. Chem. Phys.* **2003**, *119*, 94–100.

(42) Wang, X. G.; Carrington, T. *J. Chem. Phys.* **2003**, *119*, 101–117.

(43) Yu, H. G. *J. Chem. Phys.* **2004**, *121*, 6334–6340.

(44) Oyanagi, C.; Yagi, K.; Taketsugu, T.; Hirao, K. *J. Chem. Phys.* **2006**, *124*, 064311.

(45) Marquardt, R.; Quack, M.; Thanopulos, I. *J. Phys. Chem. A* **2000**, *104*, 6129–6149.

(46) Ulenikov, O. N.; Bekhtereva, E. S.; Grebneva, S. V.; Hollenstein, H.; Quack, M. *Phys. Chem. Chem. Phys.* **2005**, *7*, 1142–1150.

(47) Ulenikov, O. N.; Bekhtereva, E. S.; Grebneva, S. V.; Hollenstein, H.; Quack, M. *Mol. Phys.* **2006**, *104*, 3371–3386.

(48) Wilmshurst, J. K.; Bernstein, H. J *Can. J. Chem.-Rev. Can. Chim.* **1957**, *35*, 226–235.

(49) Olson, W. B.; Plyler, E. K.; Allen, H. C. *J. Res. Natl. Bur. Stand. Sect. A-Phys. Chem.* **1963**, *67*, 27.

(50) Morillon-Chapey, M.; Alamichel, C. *Can. J. Phys* **1973**, *51*, 2189–2196.

(51) Deroche, J. C.; Guelachvili, G. *J. Mol. Spectrosc.* **1975**, *56*, 76–87.

(52) Deroche, J. C.; Graner, G.; Cabana, A. *J. Mol. Spectrosc.* **1975**, *57*, 331–347.

(53) Deroche, J. C.; Pinson, P. *J. Mol. Spectrosc.* **1975**, *58*, 229–238.

(54) Deroche, J. C.; Graner, G.; Bendtsen, J.; Brodersen, S. *J. Mol. Spectrosc.* **1976**, *62*, 68–79.

(55) Akiyama, M.; Nakagawa, T.; Kuchitsu, K. *J. Mol. Spectrosc.* **1977**, *64*, 109–124.

(56) Ulenikov, O. N.; Malikova, A. B.; Shevchenko, G. A.; Guelachvili, G.; Morillon-Chapey, M. *J. Mol. Spectrosc.* **1991**, *149*, 160–166.

(57) Ulenikov, O. N.; Malikova, A. B.; Shevchenko, G. A.; Guelachvili, G.; Morillon-Chapey, M. *J. Mol. Spectrosc.* **1992**, *154*, 22–29.

(58) Ulenikov, O. N.; Malikova, A. B.; Guelachvili, G.; Morillon-Chapey, M. *J. Mol. Spectrosc.* **1993**, *159*, 422–436.

(59) Ulenikov, O. N.; Tolchenov, R. N.; Koivusaari, M.; Alanko, S.; Anttila, R. *J. Mol. Spectrosc.* **1994**, *167*, 109–130.

(60) Ulenikov, O. N.; Hirota, E.; Akiyama, M.; Alanko, S.; Koivusaari, M.; Anttila, R.; Guelachvili, G.; Tolchenov, R. N. *J. Mol. Spectrosc.* **1996**, *180*, 423–432.

(61) Hollenstein, H.; Marquardt, R.; Quack, M.; Suhm, M. A. *Ber. Bunsenges. Phys. Chem.* **1995**, *99*, 275–281.

(62) Signorell, R.; Marquardt, R.; Quack, M.; Suhm, M. A. *Mol. Phys.* **1996**, *89*, 297–313.

(63) Albert, S.; Bauerecker, S.; Boudon, V.; Brown, J. M.; Champion, J. P.; Loete, M.; Nikitin, A.; Quack, M. *Chem. Phys.* **2009**, *356*, 131−148.

(64) Niederer, H. M.; Albert, S.; Bauerecker, S.; Boudon, V.; Champion, J. P.; Quack, M. *Chimia* **2008**, *62*, 273–276.

(65) Hippler, M.; Quack, M. *J. Chem. Phys.* **2002**, *116*, 6045–6055.

(66) Quack, M. *Chimia* **2003**, *57*, 147–160.

(67) Albert, S.; Albert, K. K.; Quack, M. *Trends in Optics and Photonics (TOPS)*; Optical Society of America: Washington DC, 2003; *Vol. 84*, pp 177−180.

(68) Albert, S.; Quack, M. *ChemPhysChem* **2007**, *8*, 1271–1281.

(69) Albert, S.; Bauerecker, S.; Quack, M.; Steinlin, A. *Mol. Phys.* **2007**, *105*, 541–558.

(70) Bauerecker, S.; Taraschewski, M.; Weitkamp, C.; Cammenga, H. K. *Rev. Sci. Instrum.* **2001**, *72*, 3946–3955.

(71) Bauerecker, S.; Taucher, F.; Weitkamp, C.; Michaelis, W.; Cammenga, H. K. *J. Mol. Struct.* **1995**, *348*, 237–241.

(72) Bauerecker, S. *Phys. Rev. Lett.* **2005**, *94*, 033404.

(73) Ulenikov, O. N.; Bekhtereva, E. S.; Bauerecker, S.; Albert, S.; Hollenstein, H.; Quack, M. High Resolution Spectroscopy and Dynamics of the Methane Molecule: CH_2D_2 Isotopomer. In *Proceedings Nineteenth Colloquium on High Resolution Molecular Spectroscopy, Salamanca, Spain, 11−16 September 2005*, Paper N10, p. 395; Bermejo, D., Doménech, J. L., Moreno, M. A., Eds.; Sociedad Española de Óptica: Salamanca, 2005; ISBN 84-609-6737-9.

(74) Maki, A. G.; Wells, J. S. *Wavenumber Calibration Tables from Heterodyne Frequency Measurements*, Volume 821 of NIST Spec. Publ. ; National Institute of Standards and Technology: Washington, 1991.

(75) Rothman, L. S.; et al. *J. Quant. Spectrosc. Radiat. Transfer* **2005**, *96*, 139–204.

(76) Bekhtereva, E. S.; Ulenikov, O. N.; Albert, S.; Bauerecker, S.; Hollenstein, H.; Quack, M. *Proceedings of the 20th Colloquium on High-Resolution Molecular Spectroscopy*, Paper L7, pp 288−289; Boudon, V., Ed.; Université de Dijon: Dijon, 2007, and in preparation..

(77) Longuet-Higgins, H. C. *Mol. Phys.* **1963**, *6*, 445–460.

(78) Quack, M. *Mol. Phys.* **1977**, *34*, 477–504.

(79) Pepper, M. J. M.; Shavitt, I.; v. Ragué Schleyer, P.; Glukhovtsev, M. N.; Janoschek, R.; Quack, M. *J. Comput. Chem.* **1995**, *16*, 207–225.

(80) Bekhtereva, E. S.; Ulenikov, O. N.; Sinitsin, E. A.; Albert, S.; Bauerecker, S.; Hollenstein, H.; Quack, M. On the semi-empirical determination of the methane potential energy surface. In *Proceedings of the 20th Colloquium on High-Resolution Molecular Spectroscopy*, Paper J30, p 268; Boudon, V., Ed.; Université de Dijon: Dijon, 2007 and in preparation.

(81) Watson, J. K. G. *Mol. Phys.* **1968**, *15*, 479–490.

(82) Luckhaus, D.; Quack, M. *Mol. Phys.* **1989**, *68*, 745–758.

(83) Lee, T. J.; Martin, J. M. L.; Taylor, P. R. *J. Chem. Phys.* **1995**, *102*, 254–261.

(84) Raynes, W. T.; Lazzeretti, P.; Zanasi, R.; Sadlej, A. J.; Fowler, P. W. *Mol. Phys.* **1987**, *60*, 509–525.

(85) Gray, D. L.; Robiette, A. G. *Mol. Phys.* **1979**, *37*, 1901–1920.

(86) Duncan, J. L.; Law, M. M. *Spectrochim. Acta, Part. A* **1997**, *53*, 1445–1457.

(87) Blunt, V. M.; Mina-Camilde, N.; Cedeno, D. L.; Manzanares, C. *Chem. Phys.* **1996**, *209*, 79–90.

(88) Quack, M. *J. Chem. Phys.* **1985**, *82*, 3277–3283.

(89) Ulenikov, O. N.; Bekhtereva, E. S.; Albert, S.; Bauerecker, S.; Hollenstein, H.; Quack, M., in preparation.

(90) Ulenikov, O. N.; Bekhtereva, E. S.; Sinitsin, E. A.; Albert, S.; Hollenstein, H.; Quack, M. On the Global Analysis of the CH_3D Rovibrational Energies. In *Book of Abstracts of the 20th International Conference on High Resolution Molecular Spectroscopy, Praha 2008*, Paper D27, p 71; Bludský, O., Pracna, P., Urban, Š., Eds.; ICT Press: Praha, 2008, ISBN 978-80-7080-689-0.

JP809839T